Accepted Manuscript

Petroleum Geoscience

Structural and lithological controls on the architecture of igneous intrusions: examples from the NW Australian Shelf

Niall Mark, Simon Holford, Nick Schofield, Christian Haug Eide, Stefano Pugliese, Douglas Watson & David Muirhead

DOI: https://doi.org/10.1144/petgeo2018-067

Received 31 May 2018
Revised 11 December 2018
Accepted 11 February 2019

Supplementary material at https://doi.org/10.6084/m9.figshare.c.4395974

To cite this article, please follow the guidance at http://www.geolsoc.org.uk/onlinefirst#cit_journal

Structural and lithological controls on the architecture of igneous intrusions: examples from the NW Australian Shelf

[1]N.J. MARK, [2]S. HOLFORD, [1]N. SCHOFIELD, [3]C.H. EIDE, [4]S. PUGLIESE, [1]D.A. WATSON, [1]D. MUIRHEAD

[1]Department of Geology and Petroleum Geology, University of Aberdeen, Aberdeen AB24 3UE, UK

[2]Australian School of Petroleum, University of Adelaide, SA 5005, Australia

[3]Department of Earth Science, University of Bergen, Box 7803, 5020 Bergen, Norway

[4]Chrysaor, Brettenham House, Lancaster Place, London WC2E 7EN

**Corresponding author (e-mail: simon.holford@adelaide.edu.au)*

ABSTRACT

Rift-related magmatism resulting in widespread igneous intrusions has been documented in various basins, including the Faroe Shetland Basin (UK), Voring and Møre Basins (Norway) and along the NW Shelf of Australia. Seismic mapping, combined with field work, has resulted in greater understanding of subsurface intrusive plumbing systems, but knowledge of emplacement style and the mechanisms by which intrusions propagate is limited. The interpretation of a 3D seismic dataset from the Exmouth sub-basin, NW Shelf Australia, has identified numerous igneous intrusions where a close relationship between intrusions and normal faults is observed. These faults influence intrusion morphology but also form pathways by which intrusions have propagated up through the basin stratigraphy. The steep nature of the faults has resulted in the intrusions exploiting them and thus manifesting as fault-concordant, inclined dykes, whereas in the deeper parts of the basin, intrusions that have not propagated up faults typically have saucer-shaped sill morphologies. This transition in the morphology of intrusions related to fault interaction also highlights how dykes observed in outcrop may link with sills in the subsurface. Our interpretation of the seismic data also reveal subsurface examples of bifurcating intrusions with numerous splays, which have previously only been studied in outcrop.

INTRODUCTION

Magmatism associated with the break-up of continents to form new ocean basins is a common feature of many rifted margins worldwide (White & McKenzie 1989; Jolley and Bell 2002; Holford *et al.,* 2013; Ellis and Stoker 2014). This magmatism can result in the emplacement of numerous igneous intrusions throughout sedimentary basins and can also cause voluminous extrusive volcanism such as flood basalts (Planke *et al.* 2000). Despite the widespread volcanic and intrusive magmatic activity associated with rifted continental margins, which is often perceived to have negative impacts on petroleum systems, these regions are a focus for hydrocarbon exploration (Schofield *et al.* 2015). Due to the exploration of many rifted margins for hydrocarbons, widespread 3D seismic reflection coverage has allowed detailed characterisation of igneous intrusion morphology and emplacement.

Previous work examining intrusions has highlighted the importance of the host rock lithology for controlling intrusion morphologies and emplacement, with intrusions into predominantly sandy lithologies showing a preference for bifurcated and chaotic morphologies, whereas intrusions into shales have a more uniform morphology (Mudge 1968; Parsons *et al.* 1992; Schofield *et al.* 2010; Eide *et al.* 2017a). The interaction of igneous intrusions and faults has also been previously documented in relation to emplacement and morphology, with the intrusions utilising the faulted planes of weakness as an emplacement pathway (Valentine & Krogh 2006; Thomson & Schofield 2008; McClay *et al.* 2013; Magee *et al.* 2013a). Despite this, few studies have highlighted both the lithological and structural control on emplacement style and morphology in one setting (Schofield *et al.* 2010; Magee *et al.* 2013a; Eide *et al.* 2017a).

Multiple igneous intrusions are well imaged within 3D seismic data from the Exmouth sub-basin and north of the Gascoyne sub-basin (Fig. 1) and form the focus of this paper. Normal faults related to Late Jurassic-Early Cretaceous rifting in the Exmouth sub-basin have been exploited by magma resulting in a complex, interconnected network of igneous intrusions. Observations of igneous intrusions in the study area indicates a preference for fault-controlled emplacement and morphology. The numerous normal faults in the Exmouth sub-basin are the dominant emplacement pathway for igneous intrusions enabling sub-vertical movement of magma through the basin. The intrusions are highly interconnected and also display bifurcating morphologies with multiple splays, which have previously only been studied in detail at outcrop scale (Eide *et al.* 2017a).

Through interpretation of 3D seismic data, we demonstrate the importance of faulting in rifted margins for controlling the movement of magma through sedimentary basins, influencing the location of intrusions, intrusion morphologies and emplacement styles. The importance of faults as a conduit for magma movement through a basin is also discussed in relation to forced fold formation. Previously undocumented bifurcating intrusions in seismic data also offer insights into subsurface lithology and mechanical properties. Finally, this work examines how intrusions and their emplacement and resultant morphologies are relevant to ongoing hydrocarbon exploration in the region.

GEOLOGICAL HISTORY OF THE CARNARVON BASIN

The study area is located on the margins of the southern Exmouth sub-basin and the northern Gascoyne sub-basin, often referred to as the Carnarvon Terrace (Fig. 1 & 2). These basins are located both offshore and onshore along the NW Shelf of Australia along the margins of the Northern and Southern Carnarvon basins (McClay *et al.* 2013) and contain up to 15km of Palaeozoic to Recent sedimentary rocks (Partington *et al.* 2003). The Exmouth sub-basin contains mainly Triassic to Jurassic strata unconformably capped by thin (<1km) package of Cretaceous and Cenozoic sediments (Partington *et al.* 2003; Tindale *et al.* 1998). The northern Gascoyne sub-basin largely contains Palaeozoic strata with Cretaceous to Recent strata unconformably overlying Silurian to Carboniferous strata, which is consistent the fill of the Southern Carnarvon Basin (Partington *et al.* 2003).

The Exmouth and northern Gascoyne sub-basins host a series of NNE-SSW trending Early Palaeozoic-age extensional, listric growth faults, which are crosscut by NW-SE trending Permian-age extensional relay zones (Partington *et al.* 2003) (Fig. 1& 2). The tectonic evolution of both sub-basins was characterised by several stages of rifting initiating along the NW Shelf in the Late

Carboniferous (Partington *et al.* 2003) (Fig. 3). Subsequent rifting in the Early Jurassic led to the formation of the Exmouth sub-basin (Mihut & Muller 1998). This was then followed by two major phases of rifting that separated Australia from India in the Late Jurassic and Early Cretaceous (Mihut & Muller 1998; Tindale *et al.* 1998; Magee *et al.* 2013a, b) (Fig. 3). The rifting generated numerous NNE to SSW-trending normal faults, whilst uplift associated with rifting resulted in a series of regional unconformities ranging in age from Late Jurassic (Callovian-Oxfordian) to Early Cretaceous (Berriasian-Valangaian) (Mihut & Muller 1998). Subsequent to rifting, the two sub-basins underwent a period of thermal sag, with deposition of Cretaceous and Cenozoic strata. During the Late Cretaceous, the study area underwent a phase of uplift and inversion which interrupted subsidence, and is interpreted to be linked to far field plate movements associated with the onset of the Tasman Sea oceanic spreading (Bradshaw *et al.* 1998). In the Neogene, a further inversion event occurred, linked to subduction and collision of the Australian and Eurasian plates (Longley *et al.* 2002; McClay *et al.* 2013).

The major rifting events during the Early Jurassic to Late Cretaceous were also linked to extensive igneous activity across the NW shelf of Australia (Symonds *et al.* 1998). This magmatic province encompasses an area 2000 km long and 500 km wide and is characterised by oceanic crust to the NW, intrusive sills and dykes, subaerial lava flows, seaward dipping reflectors and seamounts (Symonds *et al.* 1998). A summary map showing the extent of this igneous activity, with reference to the study area, is shown in Fig. 2. The causes of this volcanic and magmatic activity is postulated to be either a plume or small-scale mantle convection (Mihut & Muller 1998; Rohrman 2013; Rohrman 2015).

EXPLORATION HISTORY OF THE STUDY AREA

The NW Shelf of Australia is an important hydrocarbon producing region, with numerous large gas fields in the Northern Carnarvon Basin (Holford *et al.* 2013) (Fig. 2). The Exmouth sub-basin has experienced considerably less exploration, and fewer hydrocarbon discoveries have been made. Over 30 wells have been drilled in our study area, with only two wells encountering hydrocarbon shows (Rough Range-1 and Parrot Hill-1, Fig. 2). The majority of the wells have been drilled onshore, with only one offshore exploration well drilled to date (Herdsman-1, drilled in 2003; Fig. 2). Herdsman-1 was drilled 45 km from the North West Cape peninsula, in water depths of 557 m, with the nearest offset well (Pendock-1) located 45 km to the south in the Gascoyne sub-basin (Fig. 2). Herdsman-1 targeted a horst block, with the Lower Cretaceous Birdsong Sandstone and the Middle Jurassic Learmonth Formation identified as the primary and secondary targets, respectively (Herdsman-1 End of Well Report). Both reservoir objectives were intersected and had good reservoir quality, but no hydrocarbons were encountered and the well was plugged and abandoned (Herdsman-1 End of Well Report). The reservoir intervals encountered within the Herdsman-1 well are less than 2 km from the nearest intrusions. Away from the wellbore location, the reservoir intervals are intruded. Despite no igneous intrusions encountered in either the Herdsman-1 or Pendock-1 wells, the intrusions could have potential implications for the petroleum system elsewhere in this area, such as reduced reservoir quality and impeded hydrocarbon migration (Holford *et al.* 2013). Further north, the onshore Yardie East-1 exploration well (Fig. 2) encountered over 20 igneous intrusions within the Upper Triassic-Upper Jurassic sedimentary sequences (Yardie East 1, End of Well Report) (Fig. 4). There are several source rocks in the region including the Upper Jurassic Dingo Claystone which is the regional source rock for the major gas fields in the Northern Carnarvon Basin (Volkmann *et al.* 1983; van Aarssen *et al.* 1996). In the Exmouth sub-basin the Upper Jurassic Dingo Claystone has been partially eroded due to the uplift and erosion during the Valanginian. Additionally, any Dingo Claystone sediments that remain are likely to be immature due to the thin post Valanginian overburden. Alternative source rocks which may be present in the area include Triassic coals and the Devonian Gneudna Formation although the presence of these is difficult to predict.

INTRUSION MORPHOLOGIES AND EMPLACEMENT MECHANISMS

Recent work on emplacement processes associated with upper-crustal intrusions has demonstrated the strong lithological control of the host rock on intrusion morphology (Kavanagh *et al.* 2006;

Magee *et al.* 2012; Schofield *et al.* 2012a; Eide *et al.* 2017a). Intrusions can be emplaced into host rock in a brittle or non-brittle fashion (Schofield *et al.* 2012a). Intrusions emplaced under brittle conditions, when the host rock sediments are well consolidated and mechanically strong, typically display features like steps and bridges (Schofield *et al.* 2012a). Schofield *et al.* (2012a) demonstrated that the identification of step morphologies in both field and seismic examples can be used to interpret the intrusion propagation direction. Intrusions emplaced under non-brittle or ductile conditions are typical of host rock sediments that are poorly consolidated, mechanically weak and heterogeneous with no dominant lithology for the intrusions to focus emplacement along; this can result in globular, peperite features and magma fingers (Schofield *et al.* 2012a; Eide *et al.* 2017a). Intrusions emplaced into homogenous mudstones will commonly result in sill morphologies which are concordant to host rock bedding, with limited transgression through strata, except at the sill wings to form saucer shaped sills (Eide *et al.* 2017a). When intrusions emplace into homogenous mudstones, this leads to the development of laterally extensive intrusions. Intrusion into thick, homogenous sand-rich sediments forms multiple thin splays which bifurcate and have a chaotic morphology (Eide *et al.* 2017a). The splay morphology is formed when magma is propagating and splitting as it attempts to find a mechanically advantageous horizon to intrude (Hutton *et al.* 2009; Eide *et al.* 2017a). The emplacement mechanism and morphologies discussed can be identified in both field and subsurface data (Bell & Butcher, 2002; Smallwood & Maresh 2002; Schofield *et al.* 2012b). 3D seismic data, in particular, is beneficial for visualising intrusion steps and magma lobes allowing for the recognition of propagation direction (Thomson & Hutton 2004; Thomson 2007; Schofield *et al.* 2012b).

The intrusion of magma into basins with pre-existing structural features demonstrates that faults can be preferentially intruded by igneous bodies (Valentine & Krogh, 2006; Thomson & Schofield, 2008; Magee *et al.* 2013a Spacapan *et al.* 2016). Magee *et al.* (2013a) note several important factors about fault-intrusion interaction, such as the juxtaposition of stratigraphic units with different mechanical properties and fault planes which can be reactivated as magma conduits. Magee *et al.* (2013a) also state that preferential emplacement of intrusions along fault planes is strongly controlled by the initial propagation direction orientation relative to the dip of the fault. For example, if an intrusion intersects the fault plane through the footwall it is more likely to crosscut the fault, whereas if it intersects the fault plane through the hanging wall it is more likely to propagate up the fault (Magee *et al.* 2013a).

DATASET AND METHODOLOGY

The Coverack 2001/2002 3D seismic reflection dataset covers an area of 878 km^2 and is located at the transition between the Exmouth sub-basin to the north and Gascoyne sub-basin to the south (Fig. 2). The data was acquired to 6 seconds TWT at 2 milliseconds sample interval, with a crossline and inline spacing of 12.5 and 15 m, respectively (2001/2 Coverack 3D Seismic Interpretation Report). For the seismic data presented here, a downward increase in acoustic impedance is represented as a negative amplitude (hard kick), displayed in blue, therefore the seabed is mapped on a trough. The majority of the intrusions are contained within the strata below the Aptian and Valanginian unconformity. Within this section, the average velocity is 3072 m/s (derived from Herdsman-1) and the dominant frequency is 22 Hz, resulting in a vertical resolution of 34 m (~17.5 m detectability). Within the Coverack 2001/2 3D data, there is one exploration well (Herdsman 1) located in the NE of the survey. The well terminates in the Middle Jurassic Learmonth Formation sandstones (Fig. 3). It is possible to make good seismic to well ties in the Cretaceous to Recent section, allowing for confident regional mapping. The accompanying Coverack 2001 2D seismic reflection survey provides greater coverage to the west of the 3D survey, though the data quality is generally poorer, and decreases significantly within the deeper Paleozoic strata. The poor quality of the Coverack 2001 2D makes it difficult to confidently tie the seismic data with the Pendock-1 exploration well (Fig. 1).

The Coverack 2001/2 3D was previously the subject of study by McClay *et al.* (2013), who characterised the igneous features in terms of intrusive or extrusive origin and broadly related them to the overall evolution of the basin. This study builds on that of McClay *et al.* (2013) through a more detailed analysis of the igneous intrusions within the survey, and in particular focuses on the relationship between igneous intrusions and faults, and the importance of this relationship as a mechanism for emplacement. Our interpretation of the seismic data has therefore focused on the igneous intrusions and the key horizons that intersect the intrusions.

Across the survey, we have mapped four key horizons that can be interpreted with confidence based on the available well data (including composite logs and end of well reports) and the quality of the seismic data. These horizons include the seabed, Top Paleogene (TP), Top Cretaceous (TK), Aptian Unconformity (KA) and the Valanginian Unconformity (VK) (Fig. 5 & 3). A Top Jurassic horizon (TJ) was also mapped but is difficult to interpret away from well control. Where possible, intra Mesozoic and possible Palaeozoic horizons were also mapped but this was grouped as Pre-Jurassic stratigraphy (PJ). Figure 4 shows an interpreted regional line across the 3D survey illustrating the quality of the data. In total, 26 individual igneous intrusions were interpreted along with 15 faults that showed evidence for interaction with intrusions (Fig. 6). Interpretative techniques including 3D visualisation, opacity rendering (Thomson & Schofield, 2008) and amplitude extractions were applied to visualise the intrusion-fault interaction. A blue–white-red colour palette was used for interpreting the seismic data, whereby an increase in impedance is expressed by a blue reflector. The igneous intrusions were mapped on a strong negative amplitude, i.e. a prominent blue reflector (Fig. 6).

The intrusions encountered within the Yardie East 1 exploration well (Fig. 4) are tholeiitic dolerites (Yardie East 1, End of Well Report) and our interpretation is that the intrusions within the Coverack 3D dataset also have a mafic composition, due to their high amplitude character. Mafic intrusions generate high amplitudes as they have high acoustic impedance relative to the surrounding host rock sediments, as a function of their high density and sonic velocities (Bell & Butcher 2002; Smallwood & Maresh 2002; Mark *et al.* 2018). The intrusions are distinguishable from other high amplitude reflectors (such as the lower Cretaceous unconformities), as they are laterally discontinuous and tend to crosscut strata-related reflectors (Bell & Butcher 2002; Smallwood & Maresh 2002, Schofield *et al.* 2017a). Where the intrusions are continuous but interconnected, they can be difficult to seismically map.

RESULTS: CHARACTERISATION OF FAULTS AND INTRUSIONS FROM SEISMIC DATA

Structural Framework

The interpreted faults which influence the intrusion morphology faults are mainly steeply dipping (~40-50°), planar, domino-style normal faults. The faults all strike NNE-SSW and typically have a vertical throw of ~0.05 s TWT (~50 m). The lateral extent of the fault planes range from 2-10 km and cross-cut stratigraphy from anything between ~300 to 1500 m. The majority of the faults dip towards the west, but there are smaller antithetic faults which dip to the east. These smaller antithetic faults typically cross-cut 0.02-0.03s TWT (~20-30 m) and have a lateral extent of ~1km. The southern margin of the survey images the Rough Range and Learmouth faults, which extend onshore to the North West Cape peninsula (Fig. 2). The Rough Range and Learmouth faults subdivide the study area into the Exmouth sub-basin to the north and the Gascoyne sub-basin to the south (Baillie & Jacobson 1995). Other regionally-important fault systems include the Penzance Fault, bordering the Penzance horst, which the Herdsman-1 exploration well tested (Partington *et al.* 2003; Herdsman-1 End of Well Report). Around large structures such as the Penzance Fault the seismic imaging tends to be distorted with multiple chaotic reflectors (Fig. 5 & 7). Throughout the whole of the Cretaceous section above the Lower Cretaceous unconformities, there is extensive polygonal faulting which terminates at the top Cretaceous horizon (Fig. 5).

Age and Distribution of Intrusions

Previous studies have established that the majority of magmatism along the NW Shelf occurred during the late Jurassic to early Cretaceous (~163 Ma to 113 Ma) (Symonds *et al.* 1998; Muller *et al.* 2002; McClay *et al.* 2013; Magee *et al.* 2013; Rohrman 2013). Mapping of the igneous intrusions in the study area reveals that the majority of them terminate below, and have possibly been peneplained by the Lower Cretaceous unconformities. This suggests an upper limit of Valanginian to Aptian age for the intrusions (139 Ma to 113 Ma), which is consistent with previous postulated ages (Symonds *et al.* 1998; Mihut & Muller 1998 Müller *et al.* 2002; McClay *et al.* 2013).

In total, 26 seismically resolvable intrusions were mapped across the study area (Fig. 6). The dimensions of these intrusions vary from 0.6 to 21 km in length, and 1 to 13 km in width. The average length and width of the intrusions is 5 km x 5 km, respectively. Smaller (<0.2 km long, ~0.2 km wide), seismically resolvable intrusions were observed but not mapped across the survey (Fig. 5d). In some instances, these smaller intrusions are connected to the main group of intrusions The majority of the intrusions are focused in the NNW corner of the survey (Fig. 6b). South of the Learmouth and Rough Range faults, within the Gascoyne sub-basin, there are no detectable intrusions (Fig. 6b). In the NNW corner of the survey, where the density of intrusions is greatest, there is also significant vertical stacking of the intrusions (Fig. 6c).

Intrusion Morphologies

The 26 intrusions mapped have been classified into two categories based on their morphology (Fig. 7a). Morphology 1 (M1) intrusions, which are mostly sills, are saucer-shaped and extend laterally through the basin, generally strata-concordant with minimal transgression of the basin fill except at the tips (wings) of the intrusions (Fig. 7b). M1 intrusions also exhibit fault-related control on their morphology (Fig. 7c). Their morphology is similar to that of saucer-shaped intrusions in the deeper sections of the basins but where the M1 intrusions intersect faults, they appear to ascend sub-vertically via the fault plane resulting in a shift from a sill-like to a dyke-like morphology. The dyke-like parts of M1 intrusions have heights of ~1.2 s TWT, which is roughly equivalent to 1.2 km and M2 intrusions are typically associated with westerly-dipping normal faults.

Morphology 2 (M2) intrusions are characterised by dendritic, bifurcating morphologies (Fig. 7d). M2 intrusions are highly interconnected and consist of multiple splays which extends up to 1 km across the basin and crosscut multiple horizons. This morphology is most common in the north-west part of the study area, where multiple intrusions are vertically stacked. The M2 intrusions are typically found in the shallower sections of the basin (between 1.5-2.5 s TWT) and appear to be focused within the Upper Jurassic stratigraphy.

The dimensions for all 26 mapped intrusions are presented graphically in Figure 8, which shows that M3 intrusions with dendritic morphologies are typically smaller than M1 intrusions.

DISCUSSION

Interaction of Intrusions with Faults

Previous work has shown that magma propagates sub-vertically as dykes when the least principal stress is horizontal and magma pressure exceeds the least principal stress (Valentine & Krogh 2006). Propagation of magma can also be controlled by the rheology of the host rocks, with mechanically weak lithologies (e.g. mudstones and shales) promoting lateral magma movement (Schofield *et al.* 2012a). In this study, it is clear that pre-existing structures have exerted significant influence on intrusion geometry. Where intrusions have intersected fault planes, they propagate along the fault plane, resulting in a inclined geometry along the fault plane. As a result, many intrusions possess the characteristics of both sills and dykes (Fig. 7). This behaviour is most commonly observed in shallow parts of the basin (< 2km depth); in the deeper parts of the basin, intrusions typically have sill geometries.

Intrusions 1 and 13 provide good examples of the interactions between magma and normal faults (Fig. 9). Intrusion 13 intersects three faults labelled X, Y & Z in Figure 9. These three faults are normal faults which dip towards the north-west. When intrusion 13 intersects fault Y it propagates up this fault, indicating an emplacement preference for exploiting pre-existing structure rather than strata controlled brittle or ductile mechanisms. The emplacement relationship between the intrusions and the faults is often complex: for example, intrusion 13 has utilised several faults as emplacement pathways. Intrusion 13 shows a complex relationship with a series of domino faults (labelled X,Y,Z in Figure 9). Intrusion 13 is observed to climb fault X then moves out of the fault plane into the hanging wall of fault Y; intrusion 13 then climbs fault Y before again moving into the hanging wall of fault Z and climbing up it (Fig. 9). Importantly, this observation indicates that a single fault will not always become the dominant emplacement pathway and it is possible for intrusions to 'stair step' by selecting multiple emplacement routes.

The intrusions in this study typically exploit faults that are dipping towards to the propagation direction of the intrusions (Magee *et al.* 2013a; Magee *et al.* 2016). Intrusions 1, 13 and 20 all exhibit this behaviour to some degree (Fig. 9). We observe that north westerly-dipping faults are most commonly exploited by magma (Fig. 10). The intrusions that propagate up faults which are not perpendicular to the dominant propagation direction are generally small splays off the major intrusions (Fig. 10). This observation indicates that faults which dip in the opposite direction to the intrusion propagation direction can also be utilised as emplacement pathways, building on the model for magma-fault interaction presented by Magee *et al* (2013).

Bifurcating Intrusions in 3D Seismic Data: Comparison to Field Relationships

Recent fieldwork studies in Jameson Land in East Greenland (Eide *et al.* 2017a), Skye in NW Scotland (Schofield *et al.* 2016) and the San Rafael Intrusive Complex, SW Utah (Mark *et al.* 2018a), have documented multiple examples of igneous intrusions that have bifurcated into thinner splays and offsets as they propagate through the host rock sediments (Fig. 11). Eide *et al.* (2017a) interpreted bifurcating morphologies to be related to host rock lithology, with bifurcating intrusions typically occurring in well-cemented, homogenous sandstone units. When propagating magma encounters a sand rich unit, it splits into multiple splays in an attempt to seek out a more mechanically favourable horizon to intrude. When the magma encounters a favourable horizon, this becomes the intrusion pathway, focusing the magma and resulting in a dominant intrusion that subsequently starves the smaller splays of magma (Eide *et al.* 2017a). Intrusion morphologies and emplacement processes are generally considered to be scale-invariant, with field observations applicable to subsurface investigations (Schofield *et al.* 2012b). However, the splays and bifurcations off the larger intrusions observed in recent field studies are thin (<5m) and thus likely difficult to resolve in subsurface seismic data. Hence, there is currently no documented evidence of these bifurcating relationships observed in seismic data (Eide *et al.* 2017a; Schofield *et al.* 2016).

In the Coverack 3D seismic dataset, it is possible to image large intrusions that bifurcate into smaller intrusions, with morphologies similar to those observed at a much smaller scales in field studies (Fig. 10). Examples of this type of morphology in seismic reflection data are limited, with most previous studies of intrusions documenting saucer-shaped morphologies, or fault climbing intrusions (Bell & Butcher 2002; Thomson & Hutton 2002; Thomson & Schofield 2008; Magee *et al.* 2013a). Bifurcating intrusions with numerous splays in the field study area, occur over distances >3 km from the source intrusion (Fig. 11). In outcrop, these intrusions have an anastomosing morphology which cross-cuts multiple stratigraphic horizons (Fig. 11). The numerous splays can laterally connect to other splays or pinch out. Where the intrusions bifurcate, they can reconnect with the main intrusion body, creating a 3D compartmentalised body of host rock (Fig. 11). Similar relationships are observed in Jameson Land, East Greenland (Eide *et al.* 2017a) and San Rafael Intrusive Complex, SW Utah (Mark *et al.* 2018a) (Fig. 11).

The strong lithological control on emplacement style and resultant morphologies documented from multiple field studies makes it possible to infer the mechanical properties of the host rocks at the time of emplacement. The bifurcating intrusions in outcrop, along with the other intrusions in the Exmouth sub-basin, were emplaced during the late Jurassic to early Cretaceous, mainly into Jurassic and Triassic-age sediments. Lithological constraints from the Herdsman-1 exploration well shows that the Middle Jurassic Learmonth Formation consists of homogenous sandstones, with a net to gross of 86% and average porosities of 26% (Herdsman-1 End of Well Report). The Herdsman-1 exploration well is within 5 km of the pervasive zone of bifurcating intrusion morphologies. We infer that this thick succession of homogenous sandstone, with limited mudstone, has resulted in the development of the complicated bifurcating intrusion morphologies with multiple splays, similar to observations of intrusion emplacement into homogenous sandstones in Jameson Land, E Greenland (Eide *et al.* 2017a) and the San Rafael Intrusive Complex, SW Utah (Mark *et al.* 2018a) (Fig. 11). Interestingly, despite the high porosities encountered in the Learmonth Formation sandstones, bifurcating morphologies are still present, indicating this morphology is primarily influenced by the lack of mudstone in the host rock.

Basin-Scale Magma Movement

In the study area, the intrusions we have mapped typically propagate from the west to east. Intrusions have facilitated lateral magma transport over distances ranging from 6-20 km. When they reach a normal fault they terminate after less than ~1 km but can ascend sub-vertically for up to 1.5 seconds TWT (~1.5 km) (Fig. 12). This fault-controlled relationship limits lateral magma transport, but facilitates sub-vertical magma transport. The transition from lateral to sub-vertical magma propagation is due to the magma intersecting a more favourable emplacement pathway. Intrusions propagating for long lateral distances has been documented in other basins such as the Faroe-Shetland Basin, where individual intrusions can be mapped over lateral distances of 40 km (Schofield *et al.* 2017a).

Based on observations of the intrusions in the study area, it is possible to infer their relationship to a broader magmatic record of the NW Shelf. The majority of the intrusions are sourced from the area to the NNW of the survey and ascend through the deeper stratigraphy to the shallower parts of the basin, climbing distances of 1-1.5 km (Fig. 6 & 12). Figure 6c demonstrates that the density of intrusions is greatest in the NNW of the study area, likely indicating proximity to the magma source. Kinematic flow direction indicators, such as intrusive steps (Schofield *et al.* 2012b), further confirm the notion that magma propagated south eastward from a deeper plumbing system to the north-west of the study area (Cuvier Abyssal Plain). This corroborates previous studies across the NW Shelf which identified seaward dipping reflectors, sub-aerial lava flows and volcanic protrusions to the NW reaffirming the hypothesis of magma input from the north-west (Symonds *et al.* 1998).

A north-westerly situated source of magma input has been suggested by Rohrman (2013), who recognised a high-velocity body in deep seismic reflection data (15-18 km depth). This high-velocity body is interpreted as being a mafic or ultramafic magma chamber, and is potentially the source for the sills and dykes in the NW Shelf (Mutter *et al.* 1989; Lorenzo *et al.* 1991; Rohrman, 2013; Rohrman 2015). No high-velocity body is observed in the Coverack 3D dataset, but all available data suggests the intrusions mapped in this study has been sourced from the high-velocity body north-west of the Exmouth sub-basin (Rohrman, 2013). The intrusions in the study area demonstrate how interconnected sills within a basin facilitate magma transport over substantial horizontal distances from the source of magma input into a basin (Schofield *et al.* 2017a; Magee *et al.* 2016), and thus examination of intrusions in isolation may not reveal the true extent of a magmatic plumbing system. The notion of significant, south-easterly directed magma transport could have important implications for the properties of the host rock sediments within the Exmouth sub-basin, with the potential for sandstone reservoirs to be mechanically and thermally altered by interconnected sill complexes.

Comparison of dyke emplacement in the subsurface and field-based studies

Traditional field-based interpretations of the relationship between sills and dykes typically assume a feeder system whereby sills are fed by deeper dykes (Chevalier & Woodford 1999; Thomson & Hutton 2004; Kavanagh *et al.* 2006), whilst dykes are usually interpreted as being emplaced entirely as vertical intrusions through the subsurface (Delaney & Pollard 1981, Gartner 1986, Kavanagh *et al.* 2006; Gill, 2010). Due to the limits of outcrop exposure, field-based studies result in only a partial understanding of the subsurface connectivity between sills and dykes, whereas 3D seismic data offers the potential to better understand these relationships. In this study, we have documented examples of sills in the deeper sections of the basin that feed shallower dykes (Fig. 13), such as intrusion 1 which propagates laterally over a distance of 6.5 km, but upon intersecting a fault, propagates sub-vertically (Fig. 13). Our observations point to an important role of faults in promoting the transitions from dominantly lateral to vertical propagation of magma to shallower crustal depths.

We note that the component of Intrusion 1 that has a dyke-like morphology is characterized by en-echelon steps at its point of termination, which we interpret as being related to the pre-existing fault structure. These en-echelon steps are clearly visible on an amplitude map of the Lower Cretaceous unconformity, where they stand out as high amplitude features (Fig. 13). The morphology of these en-echelon steps is analogous to field examples of en-echelon dykes observed in the San Rafael Intrusive Complex, SW Utah, though the features we describe in the seismic data are larger in scale, with offsets of 100-200 m between steps (compared to the San Rafael where the offset distances range from 30-50 m; Fig. 13). These findings further demonstrate the scale-invariant nature of intrusion morphologies and processes (McCaffrey & Petford 1997; Schofield *et al.* 2012b). This observation highlights that despite the quality of field exposures, it is likely that dykes in outcrop cannot be treated as completely vertical features and could propagate laterally in the subsurface. At greater depths, dykes can become less inclined and then eventually have geometries more resembling a sill.

Apparent lack of forced folding above sills

A notable feature of the intrusions in this study is the lack of accompanying forced folding of the overburden. Forced folding is understood to be caused by doming of the overburden as a result of the emplacement of intrusions into the host rock sediments (Hansen and Cartwright 2006; Magee *et al.* 2017). Forced folds above intrusions have proven important in other basins such as the Faroe Shetland Basin and UK Rockall, as identification of forced folds and onlap of sediments onto the paleo-seafloor/surfaces above the sills can be used as a method of dating intrusion emplacement where radiometric age constraints are not available (Trude 2004; Hansen & Cartwright 2006; Schofield *et al.* 2017a). Unfortunately, the lack of forced folds in the Exmouth sub-basin makes determining the age of emplacement difficult.

The lack of forced folding above intrusions in the Exmouth sub-basin could be linked to the strong fault control on intrusion emplacement. The presence of faults would allow the intrusions to exploit these pathways and negate the need for mechanical uplift and expansion of the host rocks to accommodate the sill emplacement.

Alternatively, the lack of forced folding in the Exmouth sub-basin could be caused by the rift-related uplift during the early Cretaceous. The majority of the intrusions within the Coverack 3D dataset terminate at the Aptian and Valanginian unconformities (Fig. 7) and is in line with previous observations (Mihut & Muller 1998; Muller *et al.* 2002; McClay *et al.* 2013; Rohrman 2013). This observation suggests that the intrusions were emplaced syn-rift and any features such as hydrothermal vents and forced folds may have been eroded due to uplift of the Exmouth sub-basin during the early Cretaceous (McClay *et al.* 2013; Rohrman 2013).

Interaction of Intrusions with Normal Faults: Comparison to other Rifted Margins

The intrusions in the Exmouth sub-basin are strongly influenced by pre-existing faults, which dictate the emplacement and morphology of the intrusions. Other volcanic rifted margins also show interaction between intrusions and faults, but the relationship between the intrusions and the faults can differ. In the Faroe Shetland Basin (UK) the majority of the intrusions are sourced from basin bounding faults and propagate laterally from the faults into the basin (Schofield *et al.* 2017a). Seismic data from the Exmouth Plateau in the Northern Carnarvon basin reveals intrusions which are contained entirely within the graben of two normal faults (Glencoe 3D Field Operations Report). The intrusion propagates laterally along the graben and also propagates up the bounding normal faults forming a saucer shaped intrusions (Fig. 14).

Detrimental Impacts of Intrusions for Hydrocarbon Exploration along the NW Shelf

Exploration in the southern part of the Exmouth sub-basin has been limited to one offshore exploration well drilled within the area covered by the 3D dataset. Despite this, the NW Shelf remains an attractive region for future exploration, as numerous large gas field are producing in the nearby Northern Carnarvon Basin (Fig. 1). The lack of well penetrations in the southern part of the Exmouth sub-basin makes assessments of the impact of the intrusions on the petroleum system challenging. However, valuable insights into the impacts of intrusions in the Exmouth sub-basin can be gained from analogue basins, where a close spatial relationship between intrusions and exploration targets is observed (e.g. the Faroe-Shetland Basin) (Schofield *et al.* 2017a). Within the Exmouth sub-basin, the strong preference for the emplacement of intrusions along faults poses a significant risk for hydrocarbon migration (Rateau *et al.* 2013; Schofield *et al.* 2017a). The Herdsman 1 well was interpreted to have failed as a result of a lack of charge, with good reservoir quality and a valid trap observed (Herdsman 1 End of Well Report). The Dingo Claystone was not encountered in the well and is therefore interpreted to be eroded by the Valanginian unconformity, potentially explaining the lack of charge. If the Dingo Claystone has indeed been eroded, then charging of any potential prospects relies on a deeper source rock such as the Triassic Mungaroo Formation or the Devonian Gneudna Formation (Fig. 3) (Herdsman-1 Geological Report; Partington *et al.* 2003). Migration of hydrocarbons generated from Triassic or Devonian source rocks along faults would be desirable to charge any Mesozoic reservoirs such as the Late Cretaceous Birdsong Sandstone, one of the main exploration targets in the Exmouth sub-basin. This migration pathway could potentially be impeded by the presence of igneous intrusions emplaced within the faults.

The Yardie East 1 exploration well, which encountered numerous intrusions, shows fluctuating vitrinite reflectance values for the section of Dingo Claystone that was intruded (Yardie East 1 End of Well Report). This indicates that there has been contact metamorphism of the sediments (Yardie East 1 End of Well Report). If there has been extensive intrusion-related heating of the Dingo Claystone, potentially the source rock could be heated sufficiently to the point that it is post mature (Holford *et al.* 2013). Alternatively, it is possible that the heating effect of the intrusions could be sufficient to push a thermally immature source rock into the oil window commencing generation of hydrocarbons (Holford *et al.* 2013; Senger *et al.* 2017).

The bifurcated intrusions (Fig. 11) identified in this study are likely to have a greater impact on the petroleum system and exploration compared to the strata-concordant intrusions or fault-controlled intrusions. Bifurcating morphologies would result in a larger area of host rock affected by the intrusions, with implications for reservoir quality or source rock potential (Fig. 15). It is also possible that bifurcating igneous intrusions with multiple splays could isolate 3D volumes of sediments, compartmentalising potential reservoirs or source rocks (Ratau *et al.* 2013: Holford *et al.* 2013) (Fig. 15). Holford *et al.* (2013) also suggests that compartmentalisation of sediments by igneous intrusions accompanied by rapid burial could result in significant undercompaction. If the intrusions are sealing, it is possible that differential lateral pressure cages may form within the intrusion bounded sediments, potentially resulting in drilling hazards (Holford *et al.* 2013). Any exploration targets which reside below the bifurcating intrusions would encounter slow drilling and risk drilling through pressure compartments (Fig. 15).

Pervasive igneous intrusions within a sedimentary basin, as observed in the Coverack 3D dataset, can present significant problems for seismic imaging (Fig. 15a). Due to the high acoustic impedance of igneous intrusions, seismic energy is attenuated and results in reduced energy transmission and consequently degrades the quality of imaging below igneous intrusions (Smallwood & Maresh 2002; Eide *et al.* 2017b; Mark *et al.* 2018a). Evaluation of any sub-intrusion prospects is thus likely to be challenging due to poor seismic imaging (Fig. 15a). The disruption of the seismic data within the Coverack 3D also makes regional interpretation of horizons away from well control difficult, which would limit understanding of the petroleum system elements. Previous work in the Faroe Shetland Basin has shown that due to the resolution limits of seismic data, thin intrusions are difficult to resolve in seismic data (Schofield *et al.* 2017a; Mark *et al.* 2018a; 2018b). Work by Schofield *et al.* (2017a) demonstrated that the majority of intrusions (88%) penetrated by wells in the FSB are less than 40 m in thickness (which is the minimum vertical resolution of the seismic data at the depths at which intrusions occur), which would make them difficult to detect in seismic data. Similarly the 20 igneous intrusions penetrated in the Yardie East-1 well range in thickness from 2 to 16 m with and average thickness of 6.1 m, indicating that many of the intrusions in the NW Shelf could potentially be difficult to detect in seismic data. This has important implications for understanding the true volumes of igneous material in a sedimentary basin, as the quantity of igneous material identifiable in seismic data is likely an underestimate (Mark *et al.* 2018a). The bifurcating intrusion morphologies observed in this study when compared to their field outcrop analogues reveals that the extent of bifurcation is much more developed, with multiple splays less than a 1 m thick (Fig. 11). It is important to consider the extent of thin splays when bifurcating intrusion morphologies are observed in seismic data, to appreciate how much additional igneous material may be present in a basin.

The numerous igneous intrusions in the Exmouth sub-basin could also have important implications for the well planning and execution phase of hydrocarbon exploration (Fig. 15). Studies focused on drilling extrusive and intrusive igneous rocks along the Atlantic Margin have highlighted multiple complications during drilling, including well instability, drilling fluid losses, slow rates of penetration (Archer *et al.* 2005; Millet *et al.* 2016), whilst additional issues such as high torque, drill bit integrity and the potential for overpressure when drilling intrusions have been anecdotally reported from numerous exploration wells (Mark *et al.* 2018a). In the Yardie East 1 well, which encountered numerous igneous intrusions, rates of penetration were much lower (<2m/hr) through the intrusion-bearing section compared to shallower overburden (Yardie East 1 End of Well Report). The 8 ½" hole (deepest section drilled), which contained most of the intrusions, had low rates of penetration and bit integrity was a problem due to the hardness of the formations (Yardie East 1 End of Well Report). Figure 14c shows a schematic illustrating the potential problems that can occur when drilling igneous intrusions in volcanic rifted margins (Mark *et al.* 2018).

Interestingly, most of the previous work focused on the drilling of igneous intrusions has focused on the implications of drilling large, strata-concordant intrusions (Archer *et al.* 2005; Millet *et al.* 2016; Mark *et al.* 2018a). In the NW Shelf the presence of pervasive, bifurcating intrusion morphologies could be more problematic. Each individual intrusive splay would cause issues with slow drilling rates, and encountering a cluster of splays would result in prolonged periods of slow drilling. Critically, the extent of the bifurcation is likely far more pronounced than visible on seismic data, with observations from field analogues demonstrating splays to be even more pervasive than what is possible to image in seismic data, with multiple intrusions less than <30 cm in thickness. Slow drilling rates through multiple intrusions splays may be comparable to drilling through multiple thin limestone stringers, which cause problems of slow rate of penetration in many sedimentary basins, such as the UK North Sea (Kelly *et al.* 1980). Additionally, thin resistive beds typically form tight spots which are difficult to run the drill string or wireline tools through, causing issues when tripping into hole and pulling out of hole. This is observed during drilling through sections containing multiple limestone stringers, but a similar situation would occur and be potentially amplified if a mass of bifurcated intrusive splays was encountered (Fig. 15c). This could result in compounding issues where multiple intrusions splays would cause slow drilling and bit wear, necessitating a bit change, which requires pulling out of hole changing the drill assembly and tripping back in. Each trip in and out of the hole would risk the drill assembly becoming stuck at the various tight spots where intrusive splays are present (Fig. 15c). Slow drilling rates and trips in and out of hole results in significant non-productive time, with a typical trip out and back in hole taking over 24 hrs. Any non-productive time will result in escalation of the drilling costs of the well and in extreme scenarios if it is not possible to make progress, a side-track may be required. Additionally, the risk of getting a drill assembly permanently stuck, requiring abandonment, has significant cost implications, especially if logging while drilling (LWD) tools are lost downhole. This can also have environmental implications if a stuck drill assembly includes nuclear-based tools, such as density-neutron LWD tools.

CONCLUSIONS

This study has presented an interpretation of a 3D seismic dataset over the Exmouth sub-basin, Australian NW Shelf, containing multiple intrusions. Our main findings are:

- Intrusions in the study area preferentially intrude faults rather than a specific lithological unit.
- The main magma propagation direction is from west to east based on kinematic flow indicators identified within intrusions, indicating a magma source to the west of the study area.
- The identification of intrusions with dendritic morphologies in seismic reflection data can provide insights into the nature of host rocks into which they are emplaced. Intrusive splays observed in outcrop appear to be common features of magma intrusion into brittle, homogenous sandstones, and in this study we identify similar features in seismic reflection data.
- It is possible to image en-echelon dykes in seismic, comparable in morphology, to onshore field observations. Our findings demonstrates that en-echelon dykes can be linked to underlying intrusions that comprise a much larger magmatic plumbing system.

- Intrusions are likely to create complications for hydrocarbon exploration including; compartmentalisation of reservoirs, drilling problems such as, difficulties in imaging sub-intrusive strata, impeded migration pathways and thermal alteration of reservoir and source rock intervals.

ACKNOWLEDGEMENTS

The lead author's PhD is funded by JX Nippon Exploration and Production (U.K) as part of the Volcanic Margin Research Consortium Phase 2. Seismic interpretation was carried out using IHS Kingdom software. This work was carried out as part of a research internship to the Australian School of Petroleum. SPH is supported by ARC Discovery Project DP160101158. Stuart Archer and Dougal Jerram are thanked for their comments which greatly improved the revisions of this paper.

REFERENCES

Archer, S.G., Bergman, S.C., Iliffe, J., Murphy, C.M. and Thornton, M., 2005. Palaeogene igneous rocks reveal new insights into the geodynamic evolution and petroleum potential of the Rockall Trough, NE Atlantic Margin. *Basin Research*, *17*(1), pp.171-201.

Baillie, P.W. & Jacobson, E., 1995. Structural evolution of the Carnarvon Terrace, Western Australia. The APPEA Journal, 35(1), pp.321-332.

Bell, B.R. & Butcher, H. (2002) On the emplacement of sill complexes: evidence from the Faroe-Shetland Basin. In: The North Atlantic Igneous Province: Stratigraphy, Tectonic, Volcanic and Magmatic Processes (Ed. by D.W. Jolly & B. Bell) Geol. Soc. London. Spec. Publ., 197, 307–329.

Bradshaw, M.T., Yeates, A.N., Beynon, R.M., BrakeL, A.T., Langford, R.P., Totterdell, J.M. & Yeung, M., 1988. Paleogeographic evolution of the North West Shelf region, in Purcell, P.G. & Purcell, R.R. (Eds), The North West Shelf of Australia: Petroleum Exploration Society of Australia Symposium, Perth, 29-53.

Chevallier, L. and Woodford, A., 1999. Morpho-tectonics and mechanism of emplacement of the dolerite rings and sills of the western Karoo, South Africa. South African Journal of Geology, 102(1), pp.43-54.

Delaney, P.T. and Pollard, D.D., 1981. Deformation of host rocks and flow of magma during growth of minette dikes and breccia-bearing intrusions near Ship Rock, New Mexico (No. 1202). USGPO,.

Eide, C.H., Schofield, N., Jerram, D.A. and Howell, J.A., 2017a. Basin-scale architecture of deeply emplaced sill complexes: Jameson Land, East Greenland. Journal of the Geological Society, 174(1), pp.23-40.

Eide, C.H., Schofield, N., Lecomte, I., Buckley, S.J. and Howell, J.A., 2018. Seismic interpretation of sill complexes in sedimentary basins: implications for the sub-sill imaging problem. *Journal of the Geological Society*, *175*(2), pp.193-209.

Ellis, D. and Stoker, M.S., 2014. The Faroe–Shetland Basin: A regional perspective from the Paleocene to the present day and its relationship to the opening of the North Atlantic Ocean. Geological Society, London, Special Publications, 397(1), pp.11-31.

Gartner, A. E., 1986, Geometry and emplacement history of a basaltic intrusive complex, San Rafael Swell and Capitol Reef areas, Utah: U.S. Geological Survey Open-File Report 86- 81, 112 p

Gill, R., 2010. Igneous rocks and processes: a practical guide. John Wiley & Sons.

Hansen, D.M. and Cartwright, J., 2006. The three-dimensional geometry and growth of forced folds above saucer-shaped igneous sills. Journal of Structural Geology, 28(8), pp.1520-1535.

Holford, S.P., Schofield, N., Jackson, C.A.-L., Magee, C., Green, P.F. & Duddy, I.R. 2013 Impacts of igneous intrusions on source and reservoir potential in prospective sedimentary basins along the western Australian continental margin. In: The Sedimentary Basins of Western Australia IV (Ed. by M. Keep & S.J. Moss), Proceedings of the Petroleum Exploration Society of Australia Symposium, Perth, WA.

Jolley, D.W. and Bell, B.R. 2002. Genesis and age of the Erlend volcano, NE Atlantic Margin. Geological Society, London, Special Publications, 197(1), pp.95-109.

Kavanagh, J.L., Menand, T. and Sparks, R.S.J., 2006. An experimental investigation of sill formation and propagation in layered elastic media. Earth and Planetary Science Letters, 245(3), pp.799-813.

Kelly Jr, J., Wells, P., Perry, G.W. and Wilkie, S.K., 1980. How using oil mud solved North Sea drilling problems. *Journal of Petroleum Technology*, *32*(06), pp.931-940.

Longley, I.M., Buessenschuett, C., Clydsdale, L., Cubitt, C.J., Davis, R.C., Johnson, M.K., Marshall, N.M., Murray, A.P., Somerville, R., Spry, T.B. and Thompson, N.B., 2002. The North West Shelf of Australia–a Woodside perspective. The sedimentary basins of Western Australia, 3, pp.27-88.

Mark, N.J., Schofield, N., Pugliese, S., Watson, D., Holford, S., Muirhead, D., Brown, R. and Healy, D., 2017. Igneous intrusions in the Faroe Shetland basin and their implications for hydrocarbon exploration; new insights from well and seismic data. Marine and Petroleum Geology.

Magee, C., Jackson, C.A.L. and Schofield, N. 2013. The influence of normal fault geometry on igneous sill emplacement and morphology. Geology, 41(4), pp.407-410.

Magee, C., Briggs, F. and Jackson, C.A., 2013. Lithological controls on igneous intrusion-induced ground deformation. Journal of the Geological Society, 170(6), pp.853-856.

Magee, C., Muirhead, J.D., Karvelas, A., Holford, S.P., Jackson, C.A., Bastow, I.D., Schofield, N., Stevenson, C.T., McLean, C., McCarthy, W. and Shtukert, O., 2016. Lateral magma flow in mafic sill complexes. Geosphere, 12(3), pp.809-841.

McClay, K., Scarselli, N. and Jitmahantakul, S., 2013. Igneous intrusions in the Carnarvon Basin, NW Shelf, Australia. In The sedimentary basins of Western Australia IV: Proceedings of the Petroleum Exploration Society of Australia Symposium: Perth, Petroleum Exploration Society of Western Australia (pp. 1-20).

Mihut, D. and Müller, R.D., 1998. Volcanic margin formation and Mesozoic rift propagators in the Cuvier Abyssal Plain off Western Australia. Journal of Geophysical Research: Solid Earth, 103(B11), pp.27135-27149.

Millett, J. M., Wilkins, A. D., Campbell, E., Hole, M. J., Taylor, R. A., Healy, D., Jerram, D. A., Jolley, D. W., Planke, S., Archer, S. G. & Blischke, A. 2016. The geology of offshore drilling through basalt sequences: Understanding operational complications to improve efficiency. Marine and Petroleum Geology, 77, 1177-1192.

Mudge, M.R., 1968. Depth control of some concordant intrusions. Geological Society of America Bulletin, 79(3), pp.315-332.

Müller, R.D., Mihut, D., Heine, C., O'Neill, C. and Russell, I., 2002. Tectonic and volcanic history of the Carnarvon Terrace: Constraints from seismic interpretation and geodynamic modelling. The Sedimentary Basins of Western Australia, 3, pp.719-740.

Partington, M., Aurisch, K., Clark, W., Newlands, I., Phelps, S., Senycia, P., Siffleet, P. and Walker, T., 2003. The hydrocarbon potential of exploration permits WA-299-P and WA-300-P, Carnarvon Basin: a case study. The APPEA Journal, 43(1), pp.339-361.

Parsons, T., Sleep, N.H. and Thompson, G.A., 1992. Host rock rheology controls on the emplacement of tabular intrusions: Implications for underplating of extending crust. Tectonics, 11(6), pp.1348-1356.

Rateau, R., Schofield, N. & Smith, M. 2013 The potential role of igneous intrusions on hydrocarbon migration, West of Shetland. Petrol. Geosci., 19, 259–272.

Rohrman, M., 2013. Intrusive large igneous provinces below sedimentary basins: An example from the Exmouth Plateau (NW Australia). Journal of Geophysical Research: Solid Earth, 118(8), pp.4477-4487.

Rohrman, M., 2015. Delineating the Exmouth mantle plume (NW Australia) from denudation and magmatic addition estimates. *Lithosphere*, 7(5), pp.589-600.

Schofield, N., Stevenson, C. and Reston, T., 2010. Magma fingers and host rock fluidization in the emplacement of sills. Geology, 38(1), pp.63-66.

Schofield, N.J., Brown, D.J., Magee, C. and Stevenson, C.T., 2012. Sill morphology and comparison of brittle and non-brittle emplacement mechanisms. Journal of the Geological Society, 169(2), pp.127-141.

Schofield, N., Heaton, L., Holford, S.P., Archer, S.G., Jackson, C.A.L. and Jolley, D.W., 2012. Seismic imaging of 'broken bridges': linking seismic to outcrop-scale investigations of intrusive magma lobes. *Journal of the Geological Society*, *169*(4), pp.421-426.

Schofield, N., Holford, S., Millett, J., Brown, D., Jolley, D., Passey, S.R., Muirhead, D., Grove, C., Magee, C., Murray, J. and Hole, M., 2017. Regional magma plumbing and emplacement mechanisms of the Faroe-Shetland Sill Complex: implications for magma transport and petroleum systems within sedimentary basins. Basin Research, 29(1), pp.41-63.

Schofield, N., Jerram, D.A., Holford, S., Archer, S., Mark, N., Hartley, A., Howell, J., Muirhead, D., Green, P., Hutton, D. and Stevenson, C., 2018. Sills in sedimentary basins and petroleum systems. In *Physical Geology of Shallow Magmatic Systems* (pp. 273-294). Springer, Cham.

Smallwood, J.R. and Maresh, J., 2002. The properties, morphology and distribution of igneous sills: modelling, borehole data and 3D seismic from the Faroe-Shetland area. *Geological Society, London, Special Publications*, *197*(1), pp.271-306.

Symonds, P.A., Planke, S., Frey, O. and Skogseid, J., 1998. Volcanic evolution of the Western Australian continental margin and its implications for basin development. In *The Sedimentary Basins of Western Australia 2: Proc. Of Pet. Expl. Soc. Of Australia Symp.,* edited by P.G. and R.R. Purcell, pp.33-54, Perth

Tindale, K., Newell, N., Keall, J. and Smith, N., 1998. Structural evolution and charge history of the Exmouth sub-basin, northern Carnarvon Basin, Western Australia. In The Sedimentary Basins of Western Australia 2: Proceedings of the Petroleum Exploration Society of Australia Symposium, Perth (pp. 447-472).

Thomson, K. and Hutton, D., 2004. Geometry and growth of sill complexes: insights using 3D seismic from the North Rockall Trough. Bulletin of Volcanology, 66(4), pp.364-375.

Thomson, K., 2007. Determining magma flow in sills, dykes and laccoliths and their implications for sill emplacement mechanisms. Bulletin of Volcanology, 70(2), pp.183-201.

Thomson, K. and Schofield, N., 2008. Lithological and structural controls on the emplacement and morphology of sills in sedimentary basins. *Geological Society, London, Special Publications*, *302*(1), pp.31-44.

Trude, K.J., 2004. Kinematic Indicators for Shallow Level Igneous Intrusions from 3D Seismic Data: Evidence of Flow Firection and Feeder Location. Geological Society, London, Memoirs, 29(1), pp.209-218.

Valentine, G.A. and Krogh, K.E. 2006. Emplacement of shallow dikes and sills beneath a small basaltic volcanic center–The role of pre-existing structure (Paiute Ridge, southern Nevada, USA). Earth and Planetary Science Letters, 246(3), pp.217-230.

White, R. and McKenzie, D., 1989. Magmatism at rift zones: the generation of volcanic continental margins and flood basalts. *Journal of Geophysical Research: Solid Earth*, *94*(B6), pp.7685-7729.

FIGURE CAPTIONS

Figure 1: Regional map of the NW Shelf study area. The distribution of igneous rocks is adapted from Symonds et al (1998). Basin outlines and faults are identified along with the main oil and gas fields in the Northern Carnarvon Basin, showing that the main petroliferous basin in the region is to the north of the study area (adapted from Offshore Petroleum Exploration Acreage Release, Australia 2014).

Figure 2: Map showing the location of the study area. The map includes the Coverack 3D and 2D survey and the location of exploration wells referred to within the paper. Basic structural elements are also included (adapted from Muller *et al.,* 2002 and Partington *et al.,* 2003). Base map adapted from Google Earth.

Figure 3: Regional stratigraphic column for the NW Shelf including the local stratigraphy encountered in the Herdsman 1 exploration well drilled on the Coverack 3D seismic (Herdsman 1 End of Well Report) Stratigraphic column and tectonic events adapted from McClay et al. (2013) and Baillie & Jacobson (1995).

Figure 4: Composite log from the Yardie East-1 well showing dolerite intrusions encountered by the well within the Dingo Claystone. The intrusions are clearly distinguishable from the sedimentary host rocks based on their geophysical log responses.

Figure 5: Regional inline across the Coverack 3D seismic dataset. Pre-Jurassic stratigraphy is difficult to interpret due to the lack of well control and reduction in seismic quality below the Lower Cretaceous. Stratigraphy determined from Herdsman-1 seismic to well tie and the Coverack 3D 2001/2 Interpretative report.

Figure 6: Seismically mapped intrusions within the Coverack 3D seismic dataset superimposed on regional structural elements. a): map of all intrusions in the Coverack 3D survey, b): stacking relationships of the intrusions, c): location of seismic line in d., d): seismic line showing examples of resolvable and detectable intrusions.

Figure 7: Seismic line showing varying intrusion types within the Exmouth sub-basin. Intrusions are defined as follows: 1) intrusions which have saucer shaped sill morphologies and propagate along fault planes as sub-vertical dykes, 2) intrusions which propagate along fault planes as dykes but they have dendritic morphologies and multiple splays. a): all intrusions morphology types displayed in a seismic section, b): M1 morphology (saucer shaped), c): M1 morphology (fault influenced), d): M2 morphology (bifurcating intrusions).

Figure 8: Graph summarising the dimensions of the seismically resolvable intrusions interpreted in the Exmouth sub-basin. Morphology type 1 intrusions have saucer shaped sill morphologies which exhibit strong fault control. Morphology 2 intrusions consists of intrusions which bifurcate and have multiple splays.

Figure 9: a): seismic line showing intrusion 13's relationship with a series of domino faults labelled as faults x, y and z. The intrusion propagates along the fault plane of fault x before moving into the fault plane of fault y and eventually into the fault plane of fault z. b): amplitude extraction along the fault plane of fault z showing how the intrusion has propagated up the fault plane (seen as the high amplitude feature), c): cartoon schematic illustrating the intrusion fault relationship.

Figure 10: Seismic section illustrating how intrusions can propagate upwards along fault plates despite them dipping in the opposite direction as the dominant magma propagation direction, a) seismic line showing intrusion propagating up SE dipping fault despite intrusion propagation direction being north-west to south-east. b) 3D image showing the intrusion surface which propagates up the fault dipping to the south-east.

Figure 11: Bifurcating intrusions with multiple splays in seismic and in the field, demonstrating the scale invariant nature of intrusion morphologies, a): seismic line showing bifurcating intrusions in the Exmouth sub-basin, b): seismic line showing the bifurcating intrusions with a NE-SW orientation, c): bifurcating intrusions in east Greenland, D): bifurcating intrusions in south east Utah.

Figure 12: Seismic section illustrating the extent of magma movement from the NNW to SSE. Intrusions 20 extends for distances over 20km. a); seismic line showing the extent of sill 20's lateral and vertical propagation, b): 3D visualisation of intrusion 20, c): map showing the extent of the propagation in reference to the southern Exmouth sub-basin.

Figure 13: Seismic section showing how en-echelon dyke patterns commonly observed in the field can also be imaged in seismic reflection data, indicating that surface expressions which would be interpreted as vertical dykes can actually link to sills in the subsurface, a): the Valanginian unconformity RMS amplitude extraction surface draped over a seismic cube showing how the surface expression of en-echelon dykes plumbs into sills, b): en-echelon dykes in the field (south east Utah), c): interpreted image. The similarities in the en-echelon dyke pattern in the field and in seismic data show how it is possible that dykes interpreted as vertical features could be linked to sills in the subsurface.

Figure 14: Seismic image showing interactions between intrusions and faults in different rifted margin basins, a): seismic line from the Faroe Shetland Basin showing intrusions being fed into the basin by faults (line modified from Schofield *et al.,* 2017a) b): seismic line from the Glencoe 3D survey in the Exmouth Plateau where intrusions are contained within horst blocks.

Figure 15: a) seismic line from the Coverack 3D demonstrating the detrimental impact that igneous intrusions can have on the quality of seismic imaging quality. b) schematic cross-section showing the various ways that intrusions may impact the petroleum system, and in particular how bifurcating intrusions can compartmentalise a potential reservoir. c) schematic cross-sections illustrating how igneous intrusions can impact drilling operations with a focus on how the bifurcating intrusions observed in this study would be problematic if encountered during drilling.

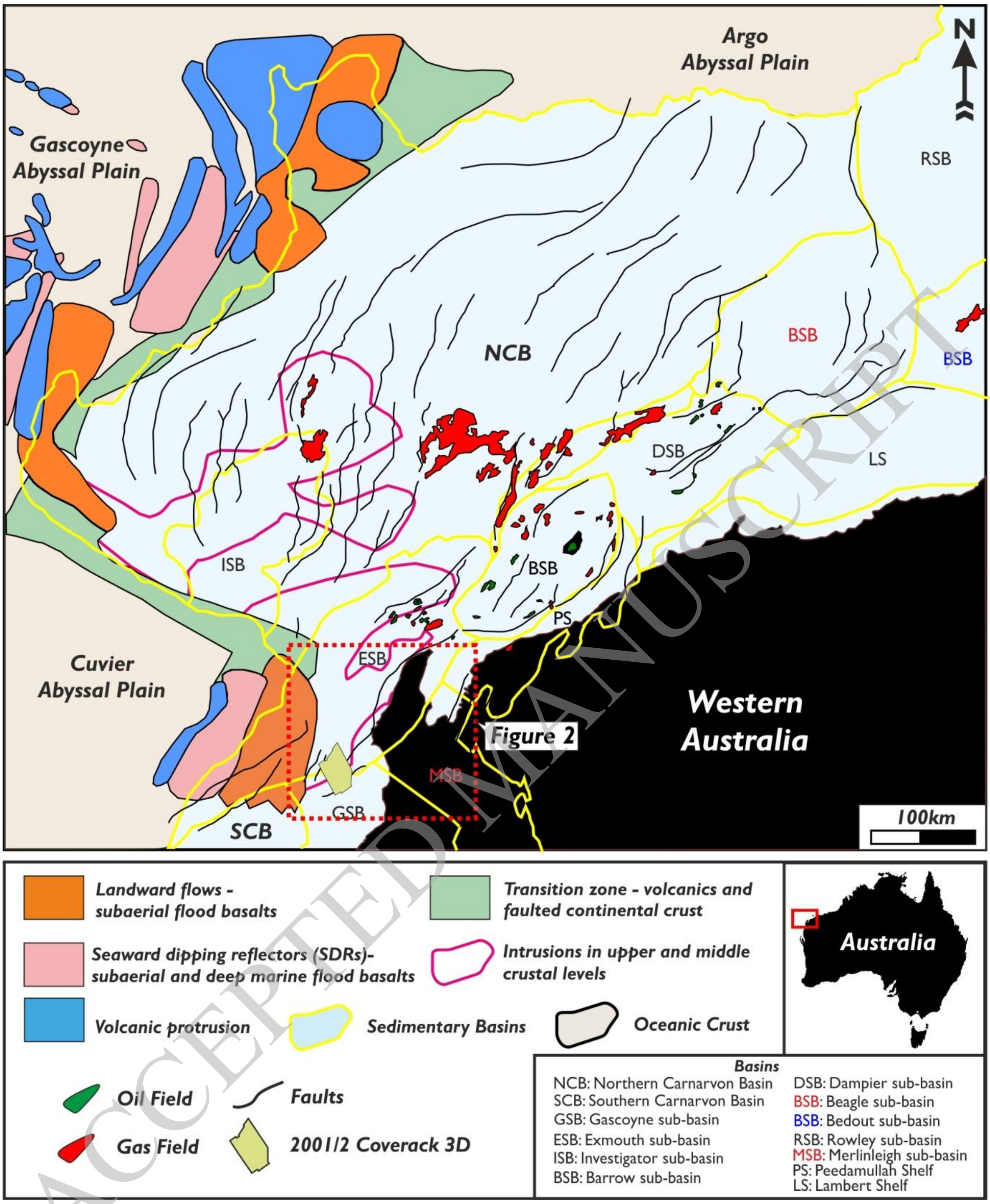
Argo Abyssal Plain
Gascoyne Abyssal Plain
Cuvier Abyssal Plain
NCB
RSB
BSB
BSB
DSB
LS
ISB
BSB
PS
ESB
MSB
GSB
SCB
Figure 2
Western Australia
100km
N
Landward flows - subaerial flood basalts
Transition zone - volcanics and faulted continental crust
Seaward dipping reflectors (SDRs)- subaerial and deep marine flood basalts
Intrusions in upper and middle crustal levels
Volcanic protrusion
Sedimentary Basins
Oceanic Crust
Australia
Oil Field
Faults
Gas Field
2001/2 Coverack 3D
Basins
NCB: Northern Carnarvon Basin
SCB: Southern Carnarvon Basin
GSB: Gascoyne sub-basin
ESB: Exmouth sub-basin
ISB: Investigator sub-basin
BSB: Barrow sub-basin
DSB: Dampier sub-basin
BSB: Beagle sub-basin
BSB: Bedout sub-basin
RSB: Rowley sub-basin
MSB: Merlinleigh sub-basin
PS: Peedamullah Shelf
LS: Lambert Shelf

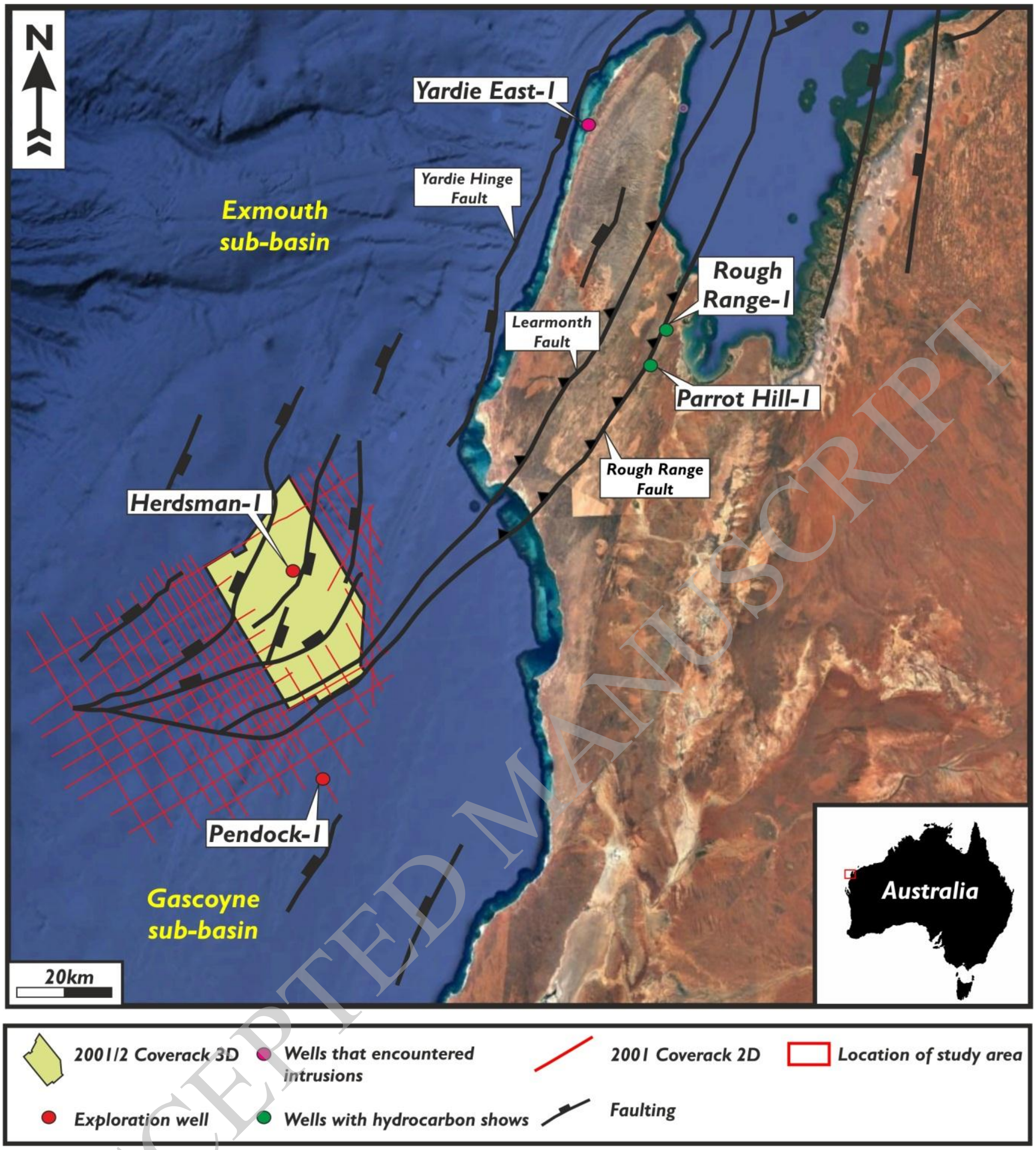
N
Yardie East-1
Yardie Hinge Fault
Exmouth sub-basin
Rough Range-1
Learmonth Fault
Parrot Hill-1
Rough Range Fault
Herdsman-1
Pendock-1
Gascoyne sub-basin
20km
Australia
2001/2 Coverack 3D
Wells that encountered intrusions
2001 Coverack 2D
Location of study area
Exploration well
Wells with hydrocarbon shows
Faulting

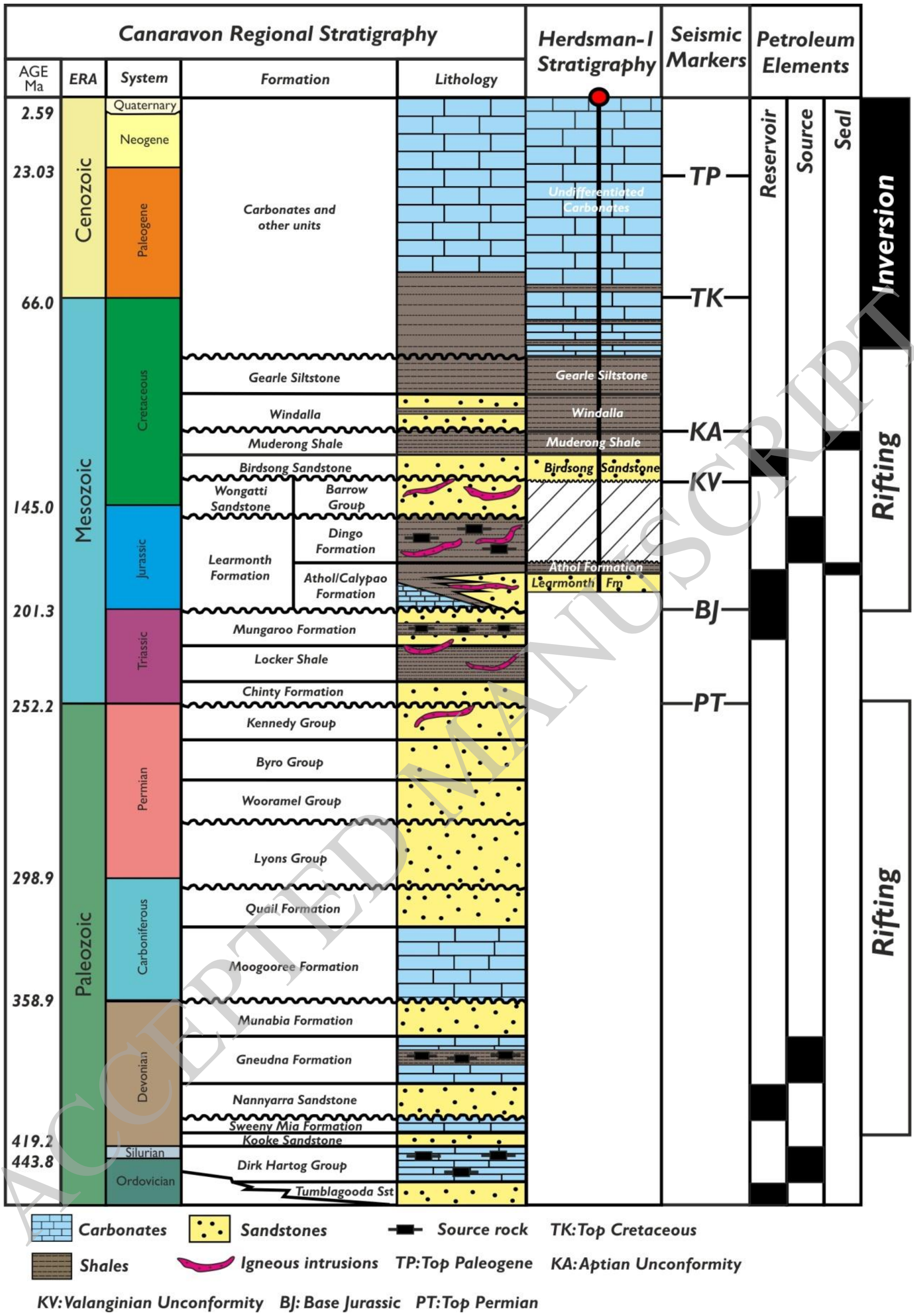
Canaravon Regional Stratigraphy
Herdsman-1 Stratigraphy
Seismic Markers
Petroleum Elements
AGE Ma
ERA
System
Formation
Lithology
Reservoir
Source
Seal
Inversion
Rifting
Rifting
2.59
23.03
66.0
145.0
201.3
252.2
298.9
358.9
419.2
443.8
Cenozoic
Mesozoic
Paleozoic
Quaternary
Neogene
Paleogene
Cretaceous
Jurassic
Triassic
Permian
Carboniferous
Devonian
Silurian
Ordovician
Carbonates and other units
Gearle Siltstone
Windalla
Muderong Shale
Birdsong Sandstone
Wongatti Sandstone
Barrow Group
Dingo Formation
Learmonth Formation
Athol/Calypso Formation
Mungaroo Formation
Locker Shale
Chinty Formation
Kennedy Group
Byro Group
Wooramel Group
Lyons Group
Quail Formation
Moogooree Formation
Munabia Formation
Gneudna Formation
Nannyarra Sandstone
Sweeny Mia Formation
Kooke Sandstone
Dirk Hartog Group
Tumblagooda Sst
Undifferentiated Carbonates
Gearle Siltstone
Windalla
Muderong Shale
Birdsong Sandstone
Athol Formation
Learmonth Fm
TP
TK
KA
KV
BJ
PT
Carbonates
Sandstones
Source rock
TK: Top Cretaceous
Shales
Igneous intrusions
TP: Top Paleogene
KA: Aptian Unconformity
KV: Valanginian Unconformity
BJ: Base Jurassic
PT: Top Permian

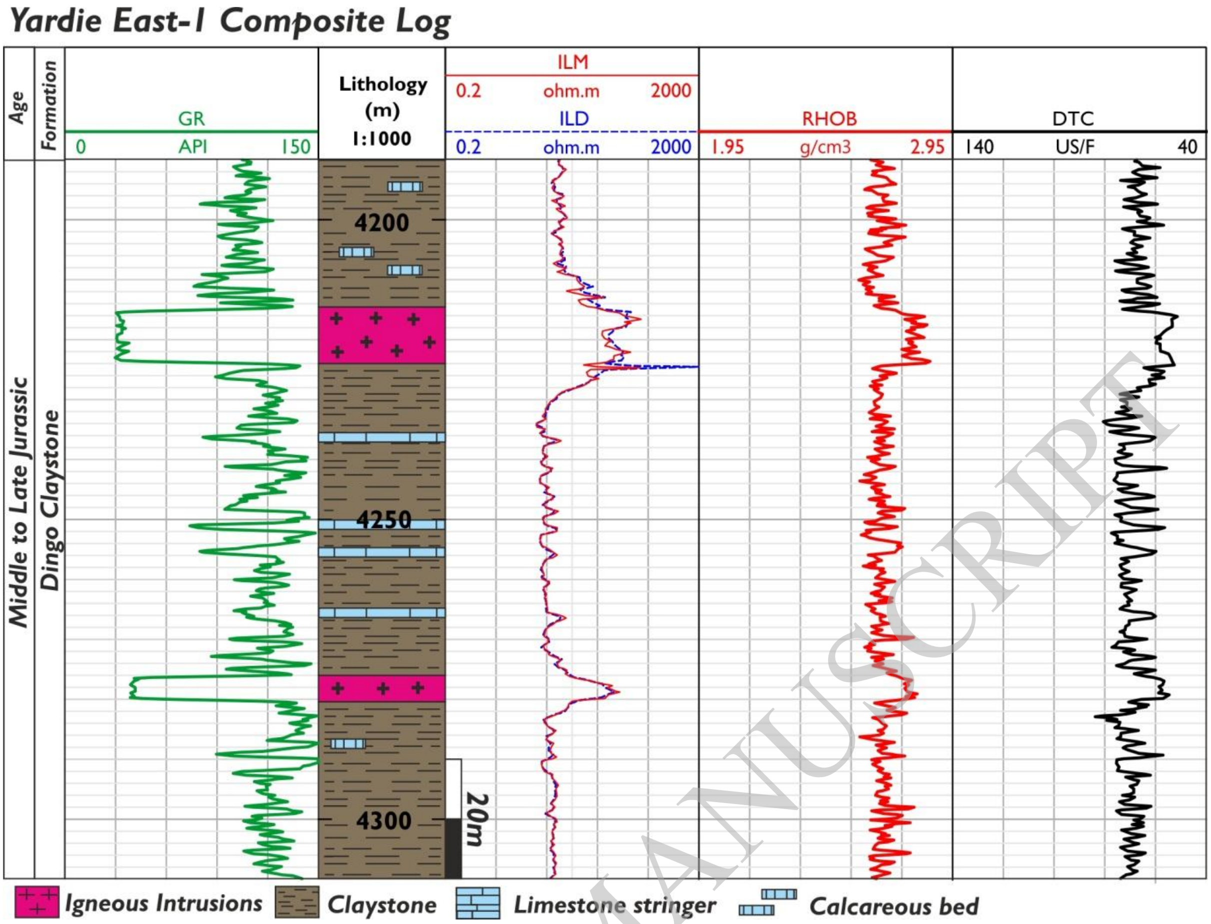
Yardie East-1 Composite Log
Age
Formation
GR
0 API 150
Lithology (m) 1:1000
ILM
0.2 ohm.m 2000
ILD
0.2 ohm.m 2000
RHOB
1.95 g/cm3 2.95
DTC
140 US/F 40
Middle to Late Jurassic
Dingo Claystone
4200
4250
4300
20m
Igneous Intrusions
Claystone
Limestone stringer
Calcareous bed

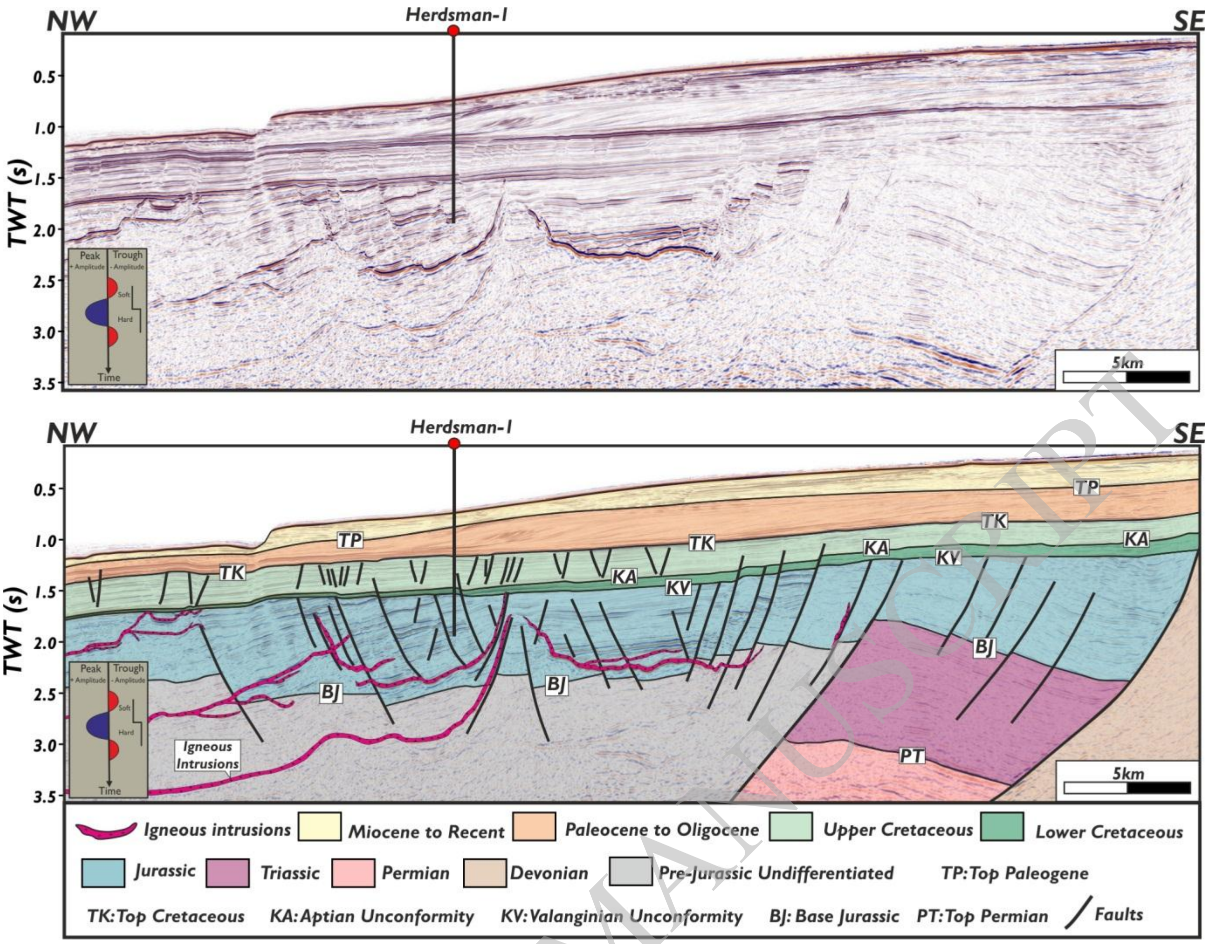
NW
Herdsman-1
SE
TWT (s)
0.5
1.0
1.5
2.0
2.5
3.0
3.5
Peak
Trough
Soft
Hard
Time
5km
NW
Herdsman-1
SE
TP
TK
KA
KV
BJ
PT
Igneous Intrusions
Igneous intrusions
Miocene to Recent
Paleocene to Oligocene
Upper Cretaceous
Lower Cretaceous
Jurassic
Triassic
Permian
Devonian
Pre-Jurassic Undifferentiated
TP:Top Paleogene
TK:Top Cretaceous
KA:Aptian Unconformity
KV:Valanginian Unconformity
BJ: Base Jurassic
PT:Top Permian
Faults

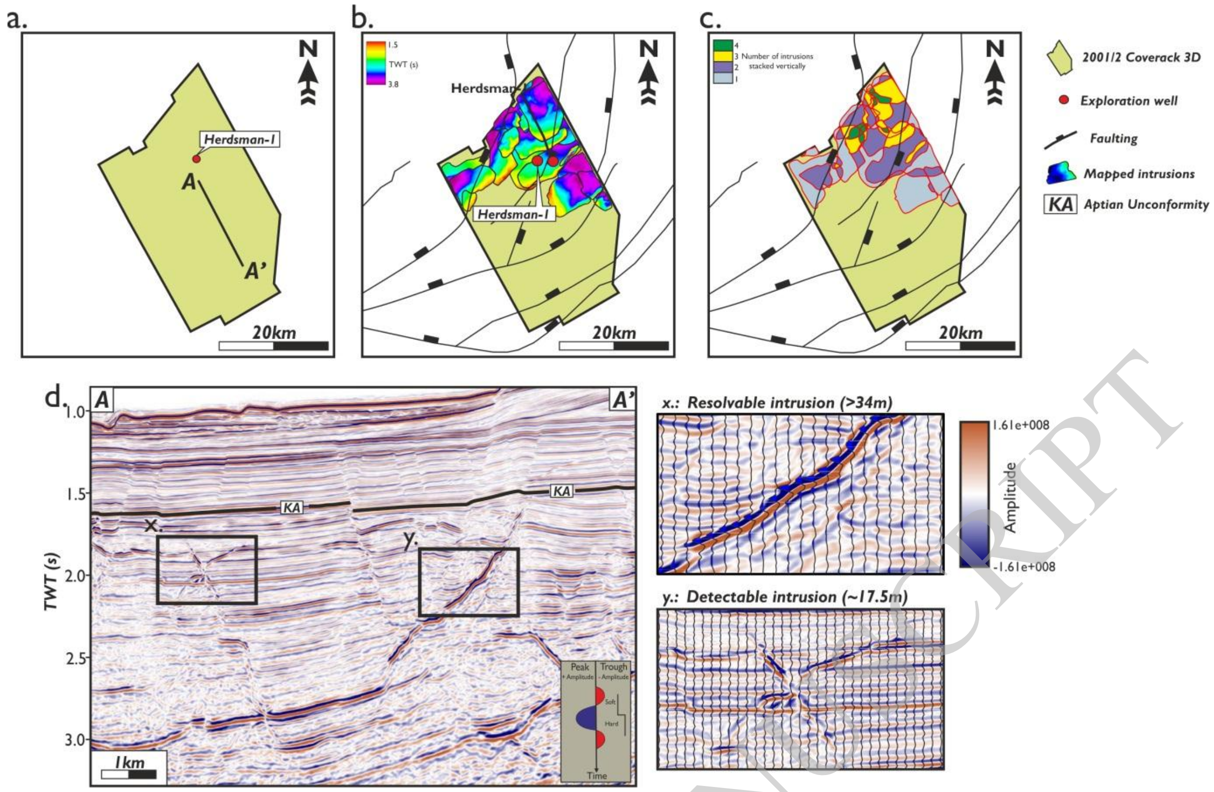
a.
b.
c.
d.
Herdsman-1
A
A'
20km
N
TWT (s)
Number of intrusions stacked vertically
2001/2 Coverack 3D
Exploration well
Faulting
Mapped intrusions
KA Aptian Unconformity
x.: Resolvable intrusion (>34m)
y.: Detectable intrusion (~17.5m)
1.61e+008
-1.61e+008
Amplitude
TWT (s)
KA
1km
Peak
Trough
Time

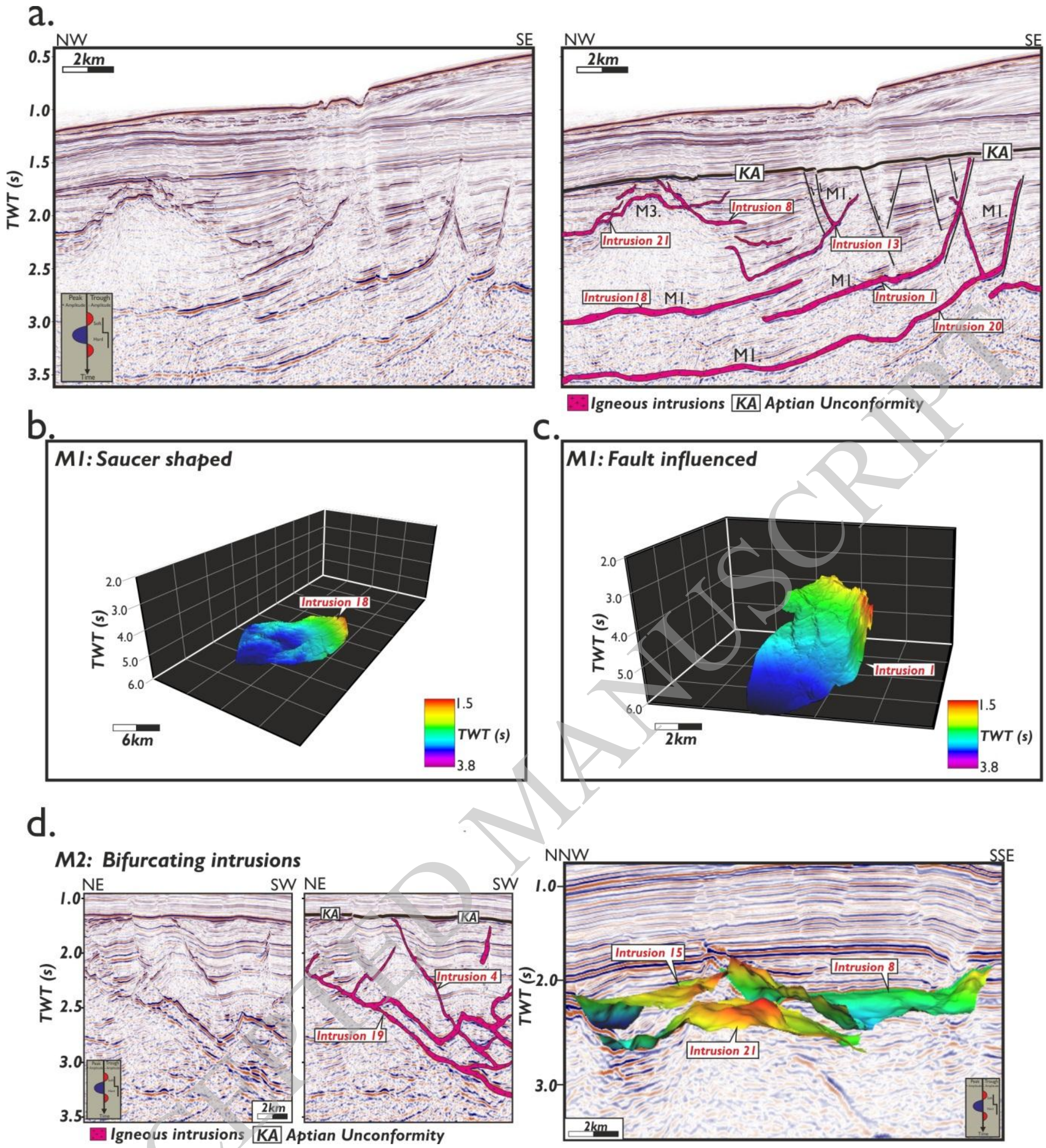

a.
NW
SE
2km
0.5
1.0
1.5
2.0
2.5
3.0
3.5
TWT (s)
KA
M3.
M1.
Intrusion 8
Intrusion 21
Intrusion 13
Intrusion18
Intrusion 1
Intrusion 20
Igneous intrusions
KA Aptian Unconformity
b.
M1: Saucer shaped
Intrusion 18
6km
TWT (s)
c.
M1: Fault influenced
Intrusion 1
2km
d.
M2: Bifurcating intrusions
NE
SW
NNW
SSE
Intrusion 4
Intrusion 19
Intrusion 15
Intrusion 21

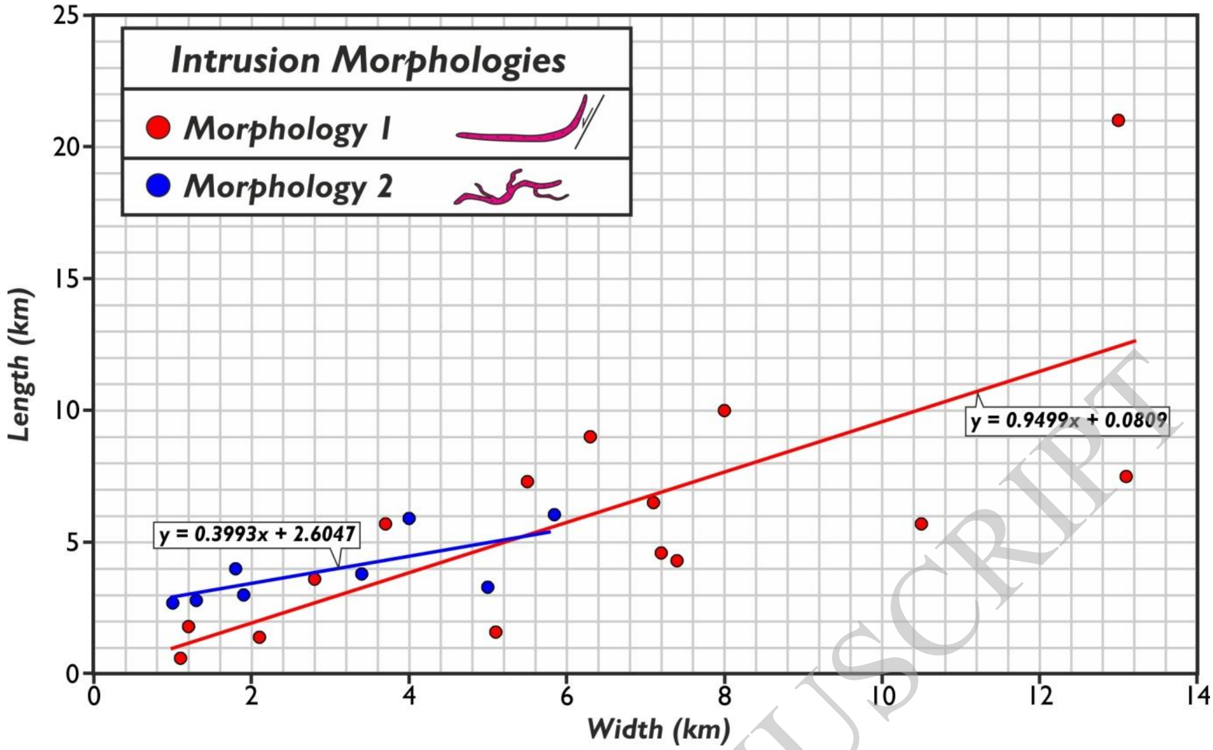
Intrusion Morphologies
Morphology 1
Morphology 2
y = 0.3993x + 2.6047
y = 0.9499x + 0.0809
Length (km)
Width (km)
25
20
15
10
5
0
0
2
4
6
8
10
12
14

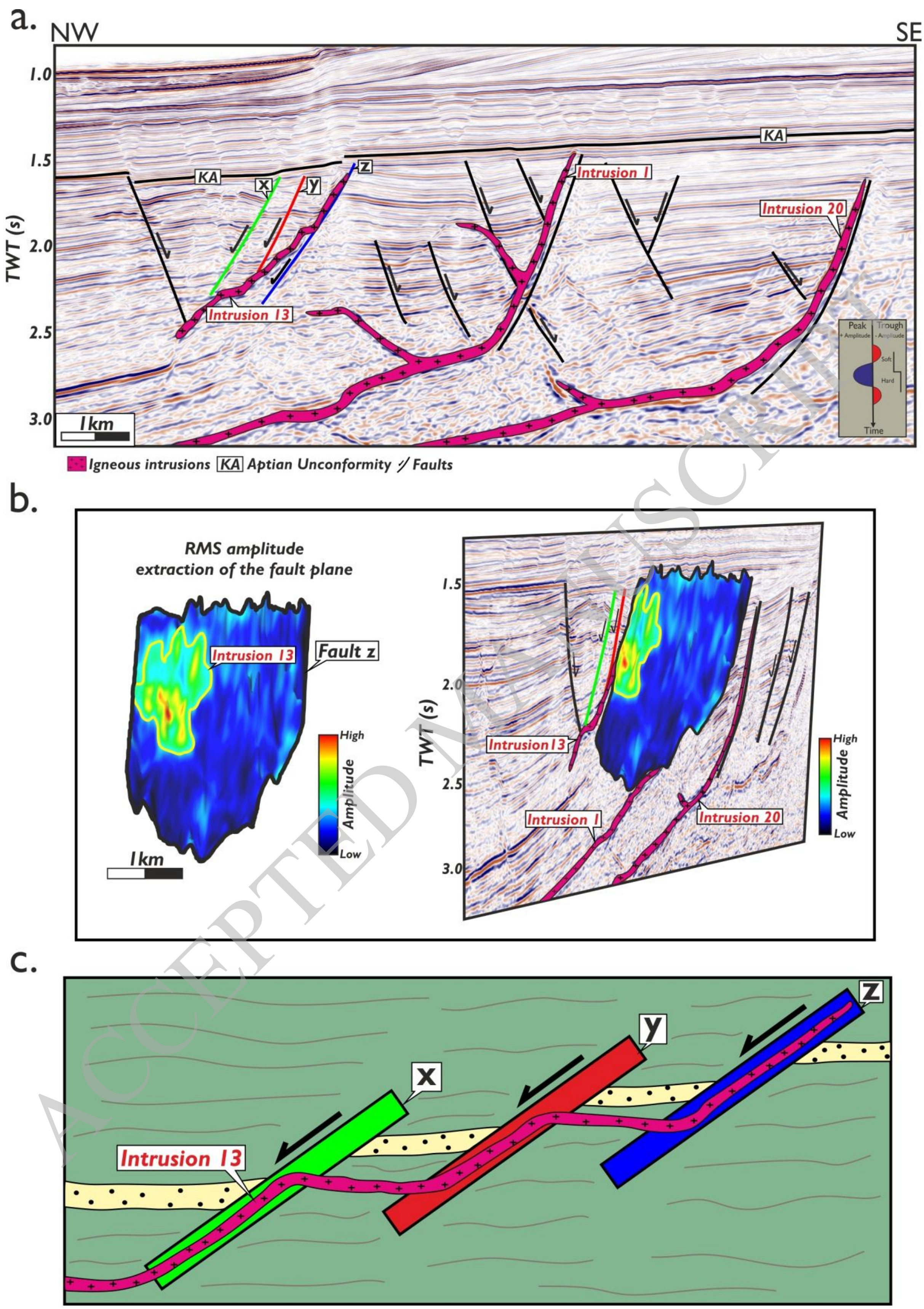
a.
NW
SE
1.0
1.5
2.0
2.5
3.0
TWT (s)
KA
x
y
z
Intrusion 1
Intrusion 20
Intrusion 13
1km
Peak
Trough
Time
Igneous intrusions
KA Aptian Unconformity
Faults
b.
RMS amplitude
extraction of the fault plane
Intrusion 13
Fault z
High
Amplitude
Low
1km
Intrusion 1
Intrusion 20
c.
x
y
z
Intrusion 13

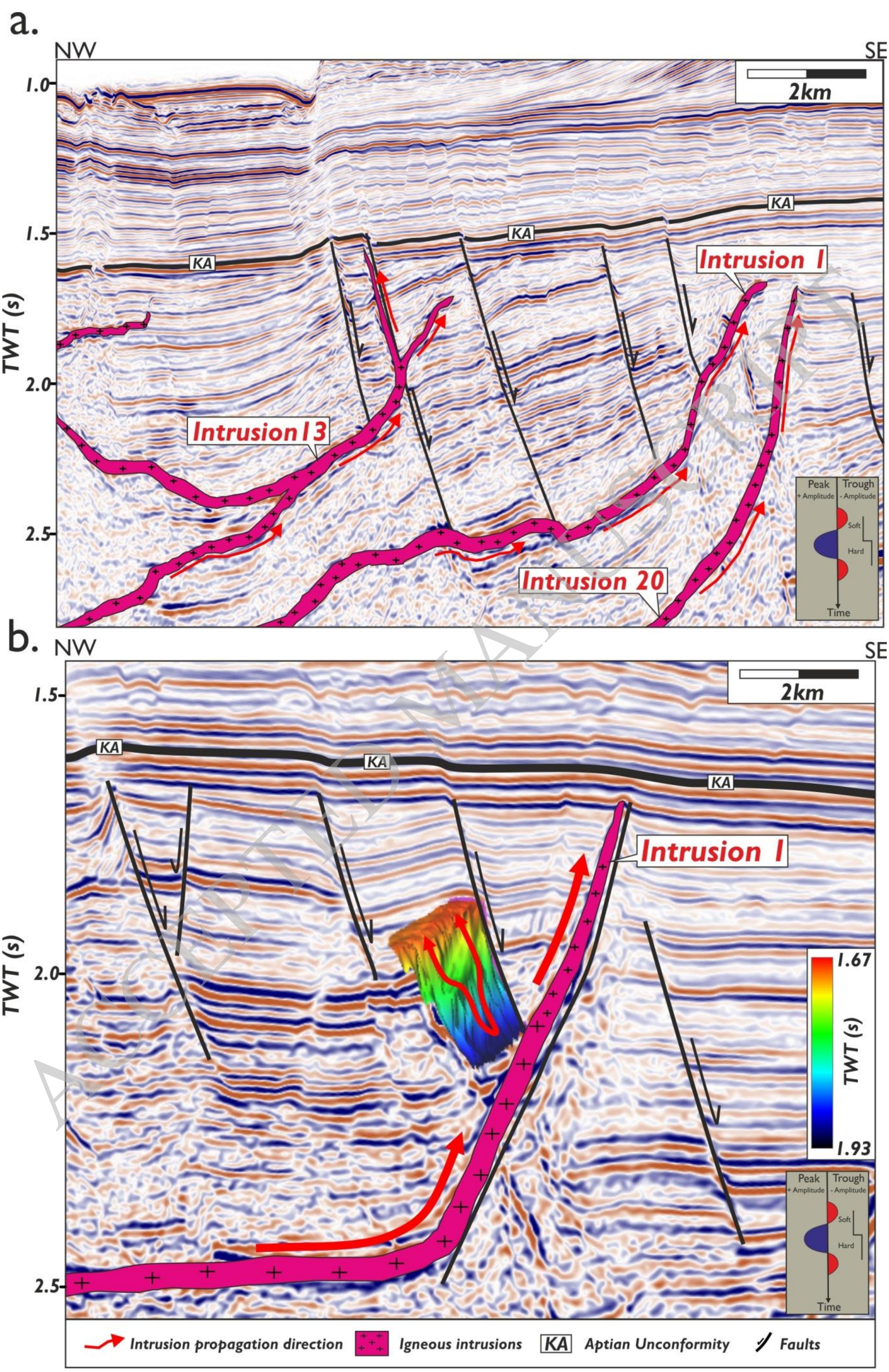

a.
NW
SE
2km
1.0
1.5
2.0
2.5
TWT (s)
KA
KA
KA
KA
Intrusion 1
Intrusion13
Intrusion 20
Peak + Amplitude
Trough - Amplitude
Soft
Hard
Time
b.
NW
SE
2km
1.5
2.0
2.5
TWT (s)
KA
KA
KA
Intrusion 1
1.67
TWT (s)
1.93
Peak + Amplitude
Trough - Amplitude
Soft
Hard
Time
Intrusion propagation direction
Igneous intrusions
KA Aptian Unconformity
Faults

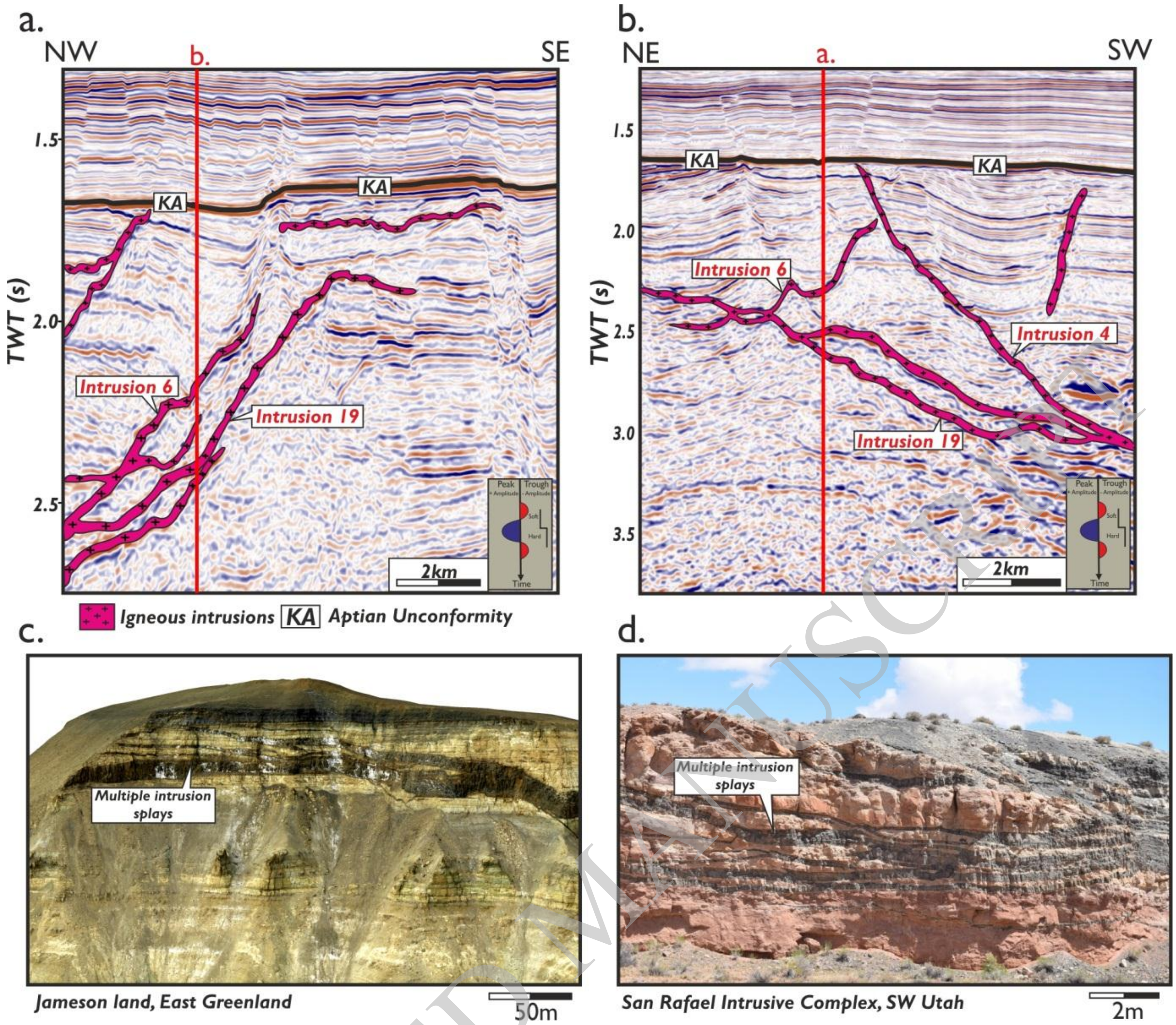
a.
NW
b.
SE
1.5
2.0
2.5
TWT (s)
KA
KA
Intrusion 6
Intrusion 19
2km
b.
NE
a.
SW
1.5
2.0
2.5
3.0
3.5
TWT (s)
KA
KA
Intrusion 6
Intrusion 4
Intrusion 19
2km
Igneous intrusions
KA
Aptian Unconformity
c.
Multiple intrusion splays
Jameson land, East Greenland
50m
d.
Multiple intrusion splays
San Rafael Intrusive Complex, SW Utah
2m

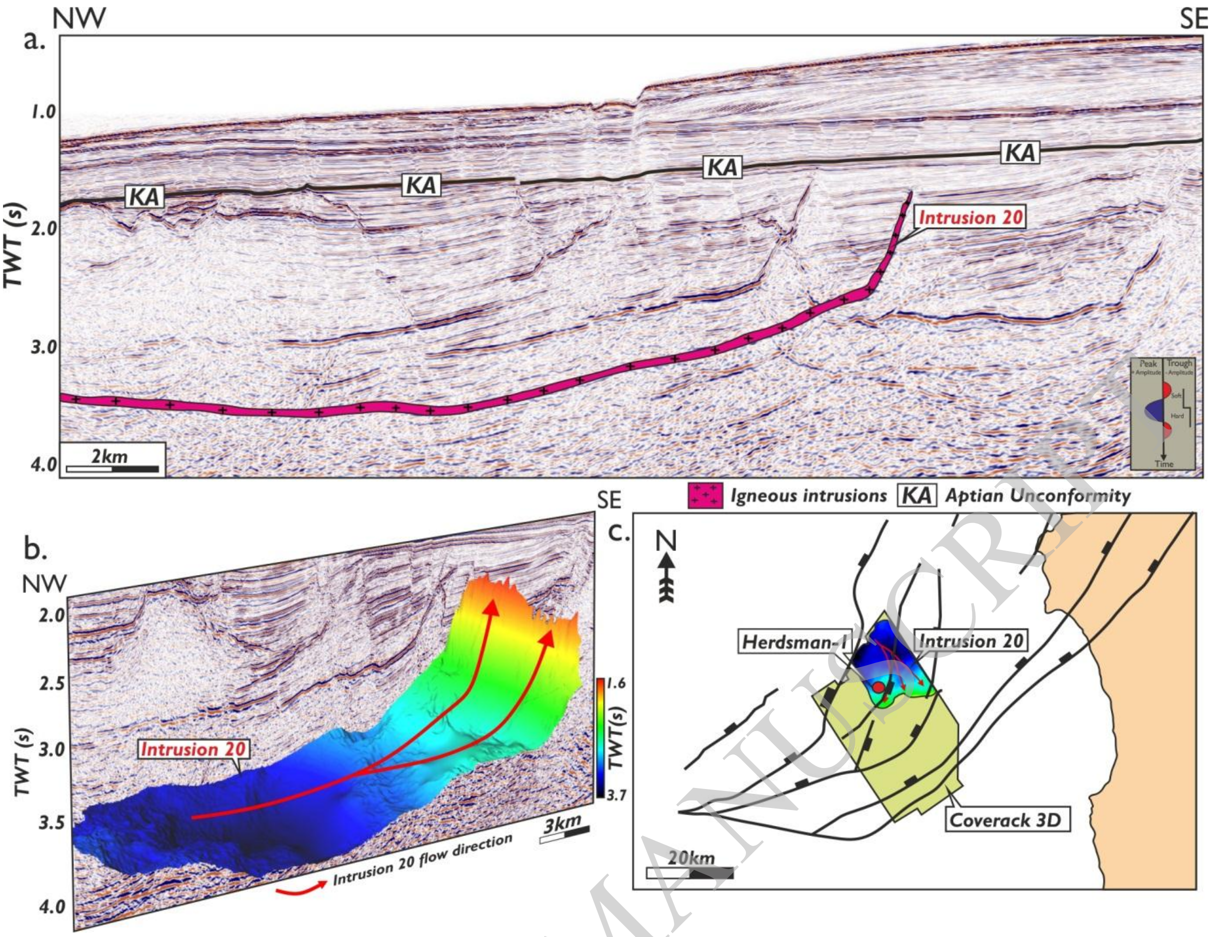

a.
NW
SE
1.0
2.0
3.0
4.0
TWT (s)
KA
KA
KA
KA
Intrusion 20
2km
b.
NW
SE
2.0
2.5
3.0
3.5
4.0
TWT (s)
Intrusion 20
1.6
3.7
TWT(s)
3km
Intrusion 20 flow direction
c.
N
Herdsman-1
Intrusion 20
Coverack 3D
20km
Igneous intrusions
KA
Aptian Unconformity

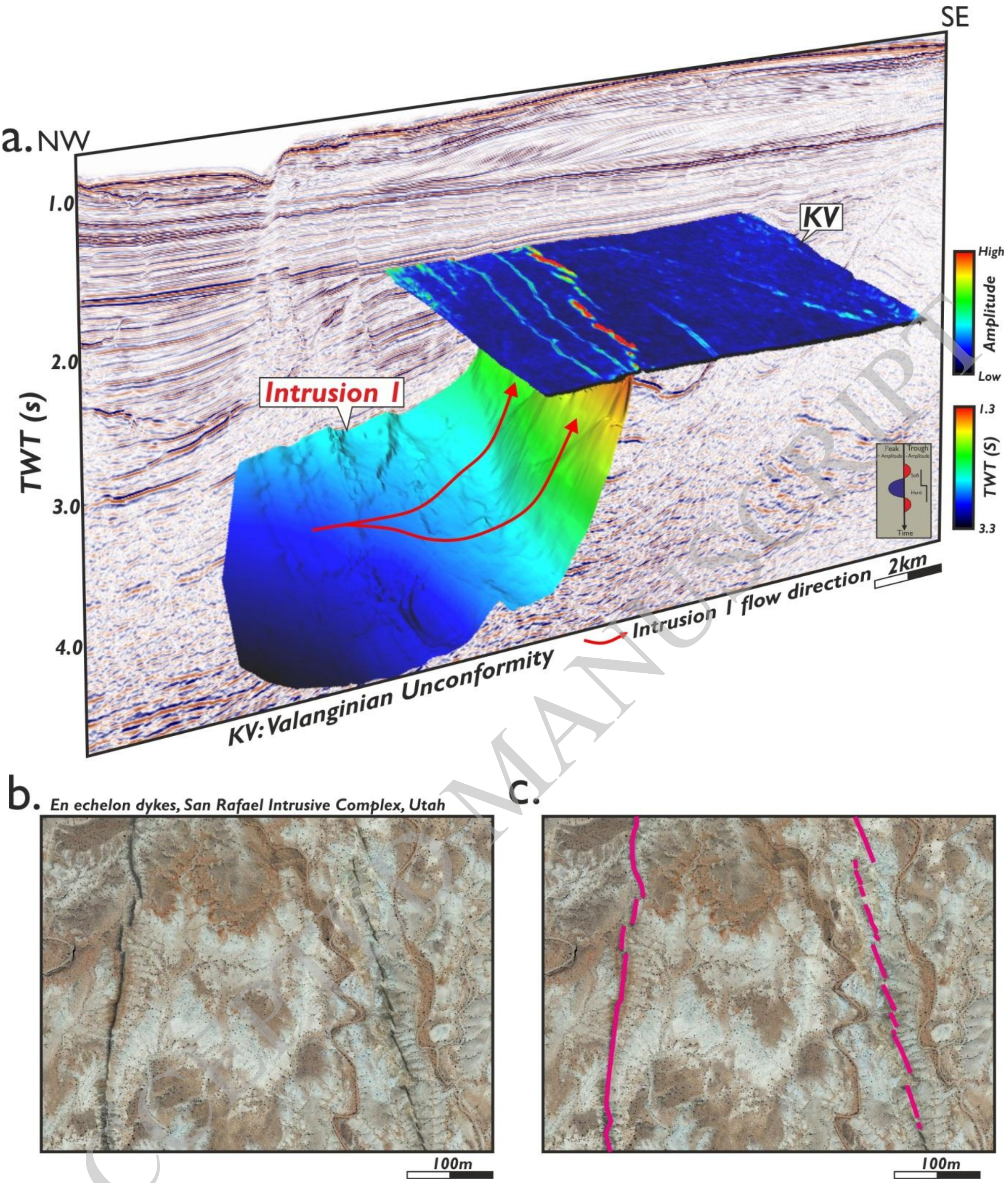
a.
NW
SE
1.0
2.0
3.0
4.0
TWT (s)
KV
Intrusion 1
High
Amplitude
Low
1.3
TWT (S)
3.3
Intrusion 1 flow direction
2km
KV: Valanginian Unconformity
b.
En echelon dykes, San Rafael Intrusive Complex, Utah
c.
100m
100m

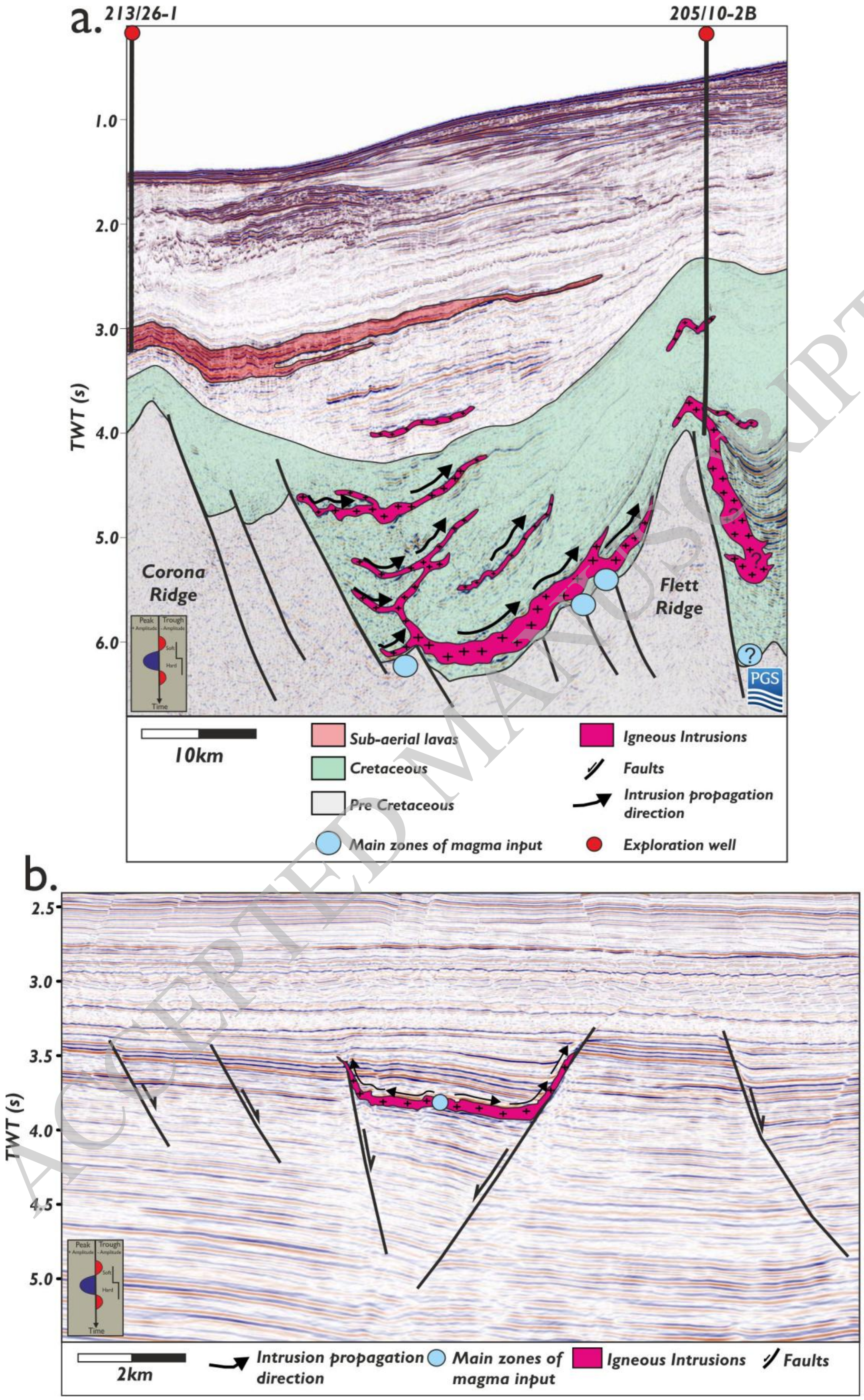
a.
213/26-1
205/10-2B
1.0
2.0
3.0
4.0
5.0
6.0
TWT (s)
Corona Ridge
Flett Ridge
PGS
10km
Sub-aerial lavas
Cretaceous
Pre Cretaceous
Main zones of magma input
Igneous Intrusions
Faults
Intrusion propagation direction
Exploration well
b.
2.5
3.0
3.5
4.0
4.5
5.0
TWT (s)
2km
Intrusion propagation direction
Main zones of magma input
Igneous Intrusions
Faults

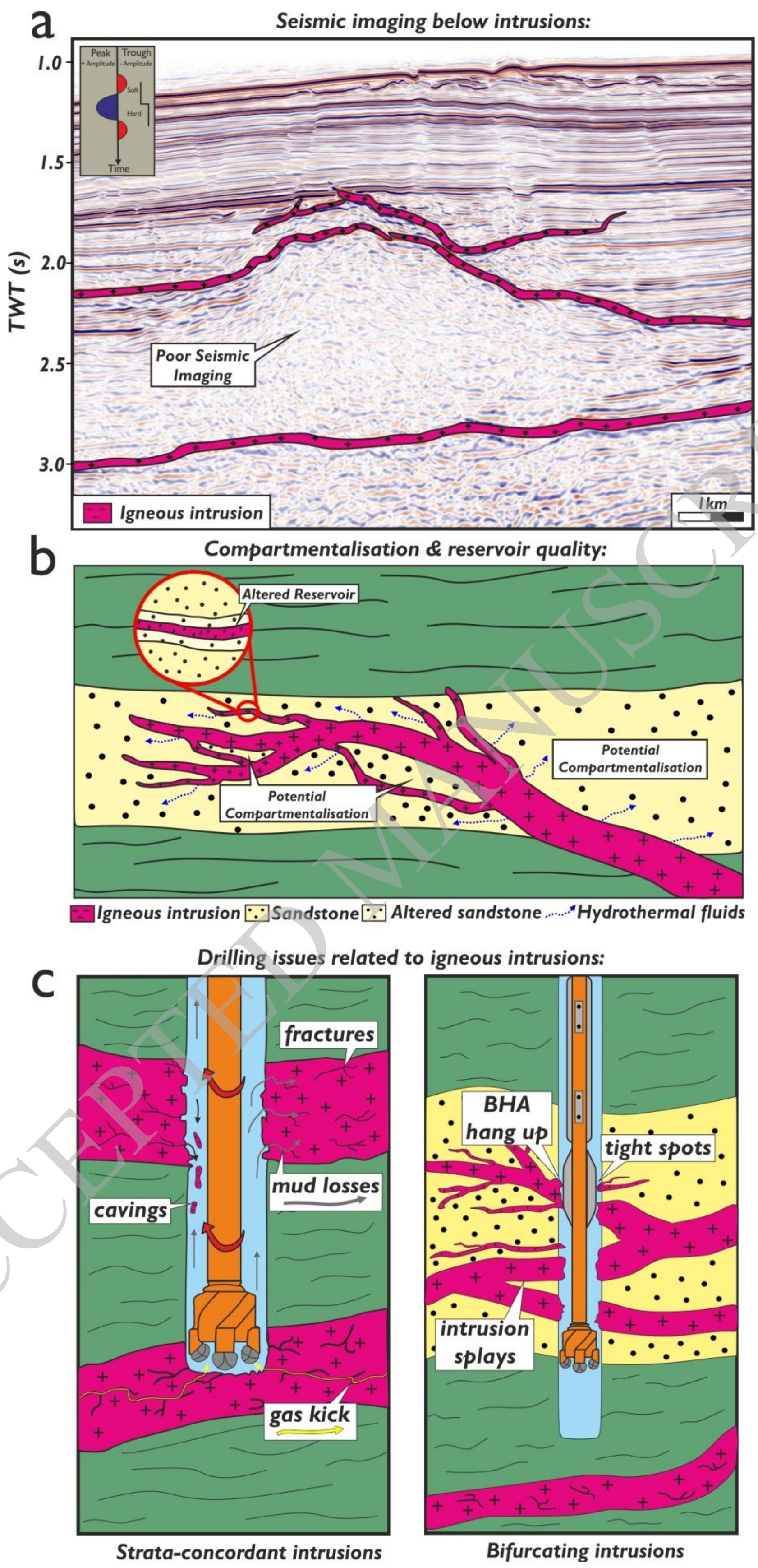

a
Seismic imaging below intrusions:
Peak
+ Amplitude
Trough
- Amplitude
Soft
Hard
Time
1.0
1.5
2.0
2.5
3.0
TWT (s)
Poor Seismic Imaging
Igneous intrusion
1km
b
Compartmentalisation & reservoir quality:
Altered Reservoir
Potential Compartmentalisation
Potential Compartmentalisation
Igneous intrusion
Sandstone
Altered sandstone
Hydrothermal fluids
c
Drilling issues related to igneous intrusions:
fractures
mud losses
cavings
gas kick
BHA hang up
tight spots
intrusion splays
Strata-concordant intrusions
Bifurcating intrusions